Version of Record: https://www.sciencedirect.com/science/article/pii/S0891584919315710
Manuscript_0cc1cd1b2caf74431cbf89ad6d9e3385

NOX4 is the main NADPH oxidase involved in the early stages of hematopoietic differentiation from human induced pluripotent stem cells

Julie Brault[a¤], Bénédicte Vigne[a¤], Mathieu Meunier[c,d], Sylvain Beaumel[a], Michelle Mollin[a], Sophie Park[c,d], Marie José Stasia[a,b]*

[a]Centre Hospitalier Universitaire Grenoble Alpes, CGD Diagnosis and Research Centre (CDiReC), Grenoble, France

[b]Univ. Grenoble Alpes, CEA, CNRS, IBS, F-38044 Grenoble, France, Grenoble, France

[c]Centre Hospitalier Universitaire Grenoble Alpes, University clinic of Hematology, Grenoble, France

[d]CNRS UMR 5309, INSERM, U1209, Université Grenoble Alpes, Institute for Advanced Bioscience, 38700 Grenoble, France

[¤]Contributed equally to the work

*Corresponding author at: Institut de Biologie Structurale, Membrane and Immunity team (MIT) Université Grenoble Alpes, 71 Avenue des Martyrs, CS 10090, F-38044 Grenoble Cedex 9

E-mail addresses: julie.brault@nih.gov (J. Brault), bvigne@chu-grenoble.fr (B. Vigne), sbeaumel@chu-grenoble.fr (S. Beaumel), mmeunier2@chu-grenoble.fr (M. Meunier), spark@chu-grenoble.fr (S. Park), mjstasia@chu-grenoble.fr (M.J. Stasia)

Graphical abstract

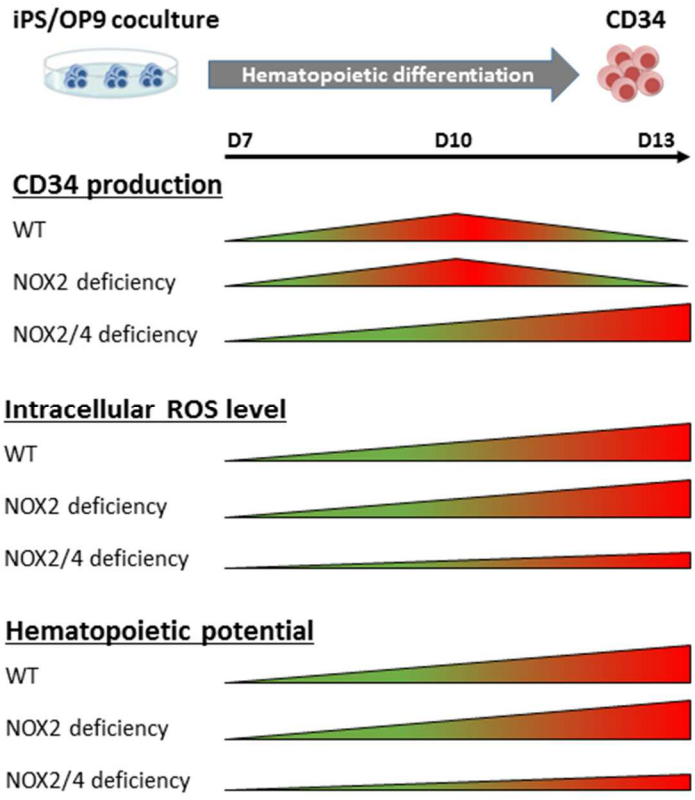

Highlights

- iPS/OP9 co-culture reproduces the *in vitro* ROS-driven maturation of $CD34^+$ progenitors
- Essential role of NOX4 in ROS production during the early stage of hematopoietic differentiation
- NOX4 can modulate the amount of $CD34^+$ production, their hematopoietic potential and phenotype
- No difference in hematopoietic differentiation between control iPSCs and NOX2-deficient iPSCs

Abstract

Reactive oxygen species (ROS) produced in hematopoietic stem cells (HSCs) are involved in the balance between quiescence, self-renewal, proliferation and differentiation processes. However the role of NOX enzymes on the early stages of hematopoietic differentiation is poorly investigated. For that, we used induced pluripotent stem cells (iPSCs) derived from X-linked Chronic Granulomatous Disease (X^0CGD) patients with deficiency in NOX2, and AR22^{0}CGD patients with deficiency in $p22^{phox}$ subunit which decreases NOX1, NOX2, NOX3 and NOX4 activity. $CD34^+$ hematopoietic progenitors were obtained after 7, 10 and 13 days of iPS/OP9 co-culture differentiation system. Neither NOX expression nor activity was found in Wild-type (WT), X^0CGD and AR22^{0}CGD iPSCs. Although NOX2 and NOX4 mRNA were found in WT, X^0CGD and AR22^{0}CGD iPSC-derived $CD34^+$ cells at day 10 and 13 of differentiation, NOX4 protein was the only NOX enzyme expressed in these cells. A NADPH oxidase activity was measured in WT and X^0CGD iPSC-derived $CD34^+$ cells but not in AR22^{0}CGD iPSC-derived $CD34^+$ cells because of the absence of $p22^{phox}$, which is essential for the NOX4 activity. The absence of NOX4 activity and the poor NOX-independent ROS production in AR22^{0}CGD iPSC-derived $CD34^+$ cells favored the $CD34^+$ cells production but lowered their hematopoietic potential compared to WT and X^0CGD iPSC-derived $CD34^+$ cells. In addition we found a large production of primitive AR22^{0}CGD iPSC-derived progenitors at day 7 compared to the WT and X^0CGD cell types. In conclusion NOX4 is the major NOX enzyme involved in the early stages of hematopoietic differentiation from iPSCs and its activity can modulate the production, the hematopoietic potential and the phenotype of iPSC-derived $CD34^+$.

Keywords: induced pluripotent stem cells, Chronic Granulomatous Disease, hematopoietic differentiation, NADPH oxidase, NOX4, reactive oxygen species.

Abbreviations: AR, autosomal recessive; CGD, Chronic Granulomatous Disease; HSCs, hematopoietic stem cells; iPSCs, induced pluripotent stem cells; NADPH, nicotinamide adenine dinucleotide phosphate; ROS, reactive oxygen species.

1. Introduction

Redox signaling is involved in a large number of cellular processes and plays an important role in stem and progenitor cells (1-3). Perturbation of the cell redox status, mainly increased levels referred as « oxidative stress », leads to various pathologies including cancer, aging, hypertension, neurodegenerative or cardiovascular diseases (4, 5). In hematopoietic stem cells (HSCs), reactive oxygen species (ROS) produced at low levels serve as secondary messengers. Thus the intracellular redox status modulates a balance between quiescence, self-renewal, migration, proliferation and differentiation processes (6-8). In consequence, a tightly regulated generation of ROS is required in order to ensure a constant pool of HSCs and a continuous production of mature blood cells through lifetime. ROS are produced from various cellular sources. Mitochondria and NADPH oxidases (NOX) are the main intracellular sources of ROS in HSCs (9-11), with half of the ROS production from NOXs (12).

The NOX family is composed of 7 isoforms (NOX1-5 and DUOX1 and 2) expressed widely in different tissues and with various roles depending on the site of expression. An increasing number of diseases has been ascribed to NOX-dependent ROS over- or under-production (13, 14). The expression of NOX1, NOX2 (also known as $gp91^{phox}$) and NOX4 membrane subunits has been previously demonstrated in peripheral blood granulocyte colony-stimulating factor (G-CSF)-mobilized $CD34^+$ cells (12, 15). NOX1 and NOX2 form a complex with the $p22^{phox}$ membrane subunit and require the presence of NOXO1 and NOXA1, or $p40^{phox}$, $p47^{phox}$ and $p67^{phox}$ cytosolic subunits respectively to produce superoxide anions $O_2^{\cdot -}$. NOX4 requires only the presence of $p22^{phox}$ and, contrary to NOX1 and NOX2, is constitutively active and produces hydrogen peroxide H_2O_2 (16, 17). In the bone marrow hematopoietic niche, the hypoxic environment regulates the NADPH oxidase activity, maintaining a low intracellular ROS level and preserving the stem cell nature of the HSCs. In contrast, an increase in ROS is associated with the differentiation and migration processes of the $CD34^+$ progenitors (6, 18). In addition NOX4 seems to exert a fundamental role in the production of ROS by embryonic stem cells (ESC)-derived $CD34^+$ cells in the context of vascular differentiation (19) as well as in hematopoietic malignancies (20, 21). However, a recent study demonstrated that ESC- and induced pluripotent stem cells (iPSC)-derived $CD34^+$ cells produced *in vitro* possess an elevated ROS level responsible for the accumulation of DNA damages and impaired progenitor ability and proliferative capacity (22).

Human iPSCs obtained after nuclear reprogramming of somatic cells have fully demonstrated their utility to model normal physiological processes and also numerous pathologies including immunological and hematopoietic diseases (23-26). The embryonic hematopoietic development can be recapitulated *in vitro* using iPSCs. Hematopoietic progenitors and mature cells like phagocytic cells are now routinely generated from iPSCs using various approaches (27-30). Chronic Granulomatous Disease (CGD) is a rare inherited disease caused by the dysfunction of the phagocytic NADPH oxidase which is unable to produce ROS, leading to recurrent and life-threatening microbial infections through life (31, 32). The main genetic form is the X-linked CGD (XCGD) caused by mutations in *CYBB* encoding NOX2. There are also rare autosomal recessive forms affecting $p22^{phox}$ (AR22CGD), $p47^{phox}$ (AR47CGD) and $p67^{phox}$ (AR67CGD). IPSC-derived from CGD patients (absence of ROS production by the NADPH oxidase) were obtained to provide *in vitro* cellular models and develop new therapeutic approaches (33-43). However, no differences were detected in the kinetic or the production yield of the mature phagocytic cells from CGD iPSCs compared to WT iPSCs. Thus, considering the major role exerted by the NADPH oxidase-driven ROS production during the hematopoietic differentiation, we hypothesized that NOX deficiency could have an impact during the early steps of differentiation mainly. We first analyzed the NOX phenotype profile of wild-type (WT), X^0CGD and $AR22^0$CGD iPSCs and iPSC-derived $CD34^+$ cells in an iPS/OP9 co-culture model of hematopoietic differentiation. Then the impact of NOX activity on the hematopoietic potential and the phenotype of the $CD34^+$ progenitors derived from WT, X^0CGD and $AR22^0$CGD iPSCs were evaluated and compared.

2. Materials and methods

2.1. Cell culture

WT-iPSCs (kindly provided by Dr T. Šarić, Institute for Neurophysiology, University of Koln, Germany), X^0CGD and $AR22^0$CGD iPSCs were reprogrammed using plasmidic vectors respectively from a healthy donor and two CGD patients as previously described (33). IPS cells were amplified in an undifferentiated state in feeder-free conditions on vitronectin (VTN; ThermoFisher)-coated plates with StemMACS™ iPS-Brew XF xeno- and serum-free medium (Miltenyi Biotec).

The mouse bone marrow stromal cell line OP9 (ATCC® CRL-2749™) was maintained on gelatinized flasks in α-MEM medium (ThermoFisher) containing 20% Fetal Bovine Serum (FBS; ThermoFisher). Four days before the induction of hematopoietic differentiation, OP9 cells were plated on gelatin-coated wells or flasks.

2.2. Hematopoietic differentiation

At day 0 of hematopoietic differentiation, iPS cells were harvested using EDTA 50 µM and small aggregates were transferred onto OP9 plates and cultured in MEM medium with 10% FBS, 100 µM

monothioglycerol (MTG; Sigma Aldrich) and 50 µg/mL ascorbic acid (AA; Sigma Aldrich) during 7, 10 or 13 days with half medium changed at day 4, 7 and 10 (43). When indicated, co-cultures were dissociated after treatment by collagenase IV during 20-25 min and trypsin-EDTA 0.05% (ThermoFisher) during 10 min and analyzed using flow cytometry, colony-forming cell assay or cell sorted. For cell sorting, cells harvested from co-cultures were labelled with CD34 magnetic beads and then isolated using AutoMACS® Pro Separator according to manufacturer's instructions (Miltenyi Biotec).

2.3. Colony-forming cell (CFC) assay

Cells obtained from co-cultures (100,000 to 500,000 cells depending on the day of co-culture) were plated in StemMACS™ HSC-CFU complete medium with erythropoietin (EPO; Miltenyi Biotec) in 35-mm Petri dishes. CFUs were scored based on their morphology after 14 days of incubation.

2.4. Phenotypic analysis by flow cytometry

Co-culture cells or CD34-sorted cells were suspended in FACS buffer (PBS, 2% FBS, 2 nM EDTA, 0.05% NaN_3) and stained with the following conjugated antibodies all purchased from Miltenyi Biotec excepted when stated otherwise: SSEA-4-fluorescein isothiocyanate (FITC) (BD Biosciences), CD34-Vioblue, CD38-phycoerythrine (PE), CD45-allophycocyanin (APC), CD90-FITC, CD117-PE-Vio770, CXCR4-PE-Vio770, CD133-Viobright FITC, CD133-APC and CD45RA-PerCP. Unconjugated antibody 7D5 directed against an external epitope of flavocytochrome b_{558} (D162-3; Clinisciences) and anti-$p22^{phox}$ (clone 44.1; Tebu Bio) with secondary antibody conjugated with AlexaFluor488 (ThermoFisher) and PE (Beckman Coulter) respectively, were used for analysis of NADPH oxidase subunit expression (44). Markers used in this study are reported in Supplementary Table 1. Control staining with appropriate isotype-matched control was included to establish thresholds for positive staining. Staining with 7-Amino-Actinomycin D (7-AAD) (BD Biosciences) was also used for dead cells exclusion. Cell fluorescence was quantified using a FACS Canto II (BD Biosciences). Data were collected and analyzed with the FACS DIVA software (BD Biosciences) and FlowJo software (Tree Star).

2.5. ROS measurements

Redox sensitive probe CellROX™ Deep Red Reagent (ThermoFisher) was used to measure the constitutive intracellular ROS production in iPS and iPSC-derived $CD34^+$ cells (45, 46). Briefly, cells pre-treated (15 min incubation at 37°C) or not with 50 µM diphenyleneiodonium (DPI) were incubated in Iscove's Modified Dulbecco's Medium (IMDM) with 5 µM CellROX™ for 30 min at 37°C, rinsed with PBS and then analyzed using a FACS Canto II (BD Biosciences). Data were collected and analyzed with the FACS DIVA software (BD Biosciences) and FlowJo software (Tree Star).

2.6. Analysis of apoptosis and necrosis

Before and after $CD34^+$ sorting with CD34 magnetic beads (Miltenyi Biotec) as previously described, hematopoietic progenitors were loaded with FITC-annexin V and propidium iodide according to the manufacturer's instructions (FITC Annexin V Apoptosis Detection Kit, BD Biosciences) and analyzed using a FACS Canto II (BD Biosciences). Data were collected and analyzed with the FACS DIVA software (BD Biosciences) and FlowJo software (Tree Star).

2.7. Western blot

Expression of NOX2, $p22^{phox}$ and NOX4 was analyzed by western blot in 50 µg of 1% Triton X100 soluble extracts prepared from human iPSCs and iPSC-derived $CD34^+$ progenitors using monoclonal antibodies 48, 449 (47) and anti-NOX4 (generous gift from Prof. U. Knaus, University Dublin, Ireland, (48)) respectively. Soluble extracts from human neutrophils (PMN) and inducible NOX4 expression in HEK-293 cells upon tetracycline [tet- and tet+, kindly provided by Prof. KH. Krause and Dr V. Jaquet University of Geneva, Switzerland (17)] were used as positive controls for NOX2/$p22^{phox}$ and NOX4 expression respectively. Polyclonal goat anti-mouse IgG-HRP was used as a second antibody and the immune complexes were detected by chemiluminescence using an ECL kit Femtomax (Rockland Immunochemicals). SDS-PAGE and immunoblotting were done at 4°C to avoid NOX4 degradation.

2.8. Molecular analysis

Total mRNA was isolated from cells using TRIzol reagent (ThermoFisher) using a modified single-step method (49) and cDNA was synthesized by the reverse transcription (RT)-PCR reaction. Then amplification by PCR was conducted with the gene-specific primers listed in Table 1. PCR was performed with β-actin primers as a control for RNA quality and equal loading. Aliquots of 2 µl of PCR products in Bromophenol Blue solution were run together with a DNA ladder (marker XIV, Roche Diagnostics) on 1% (w/v) agarose. The bands were photographed under UV light (GelDoc XR+, Bio-Rad Laboratories).

2.9. Statistical analysis

Statistical analyses were performed using GraphPad Prism 5 Software. Data are presented as mean values ± standard errors of the means (SEM). One-way ANOVA analysis of variance was used to determine the differences between multiple groups, followed by Tukey's *post hoc* multiple comparison test. Unpaired two-tailed Student's *t*-test was used for comparison between two groups.

3. Results

3.1. Kinetic and efficacy of the hematopoietic differentiation of X^{0}CGD and AR22^{0}CGD iPSCs

We previously showed that a peak of CD34$^+$ cells was obtained after 10 days of iPS/OP9 co-culture when iPSCs were first amplified on irradiated mouse embryonic fibroblasts (MEFs) (33). However, in an attempt to optimize the culture condition toward more defined culture supports, we first confirmed that the efficiency of the hematopoietic differentiation was not significantly different between WT iPSCs amplified on feeder cells (iPSCs-MEFs) or on vitronectin (iPSCs-VTN) using adapted medium before the induction of the differentiation (Fig. 1A, B and C). IPSCs-VTN cultured in xeno-free defined medium showed a slight retardation of differentiation at day 7 compared to iPSCs-MEFs cultured with a typical medium containing serum (Fig 1B and C), but at the two later time points the two culture conditions displayed similar kinetics and efficiency of differentiation. Thus iPS cells can be amplified in feeder-free conditions without affecting their hematopoietic differentiation ability.

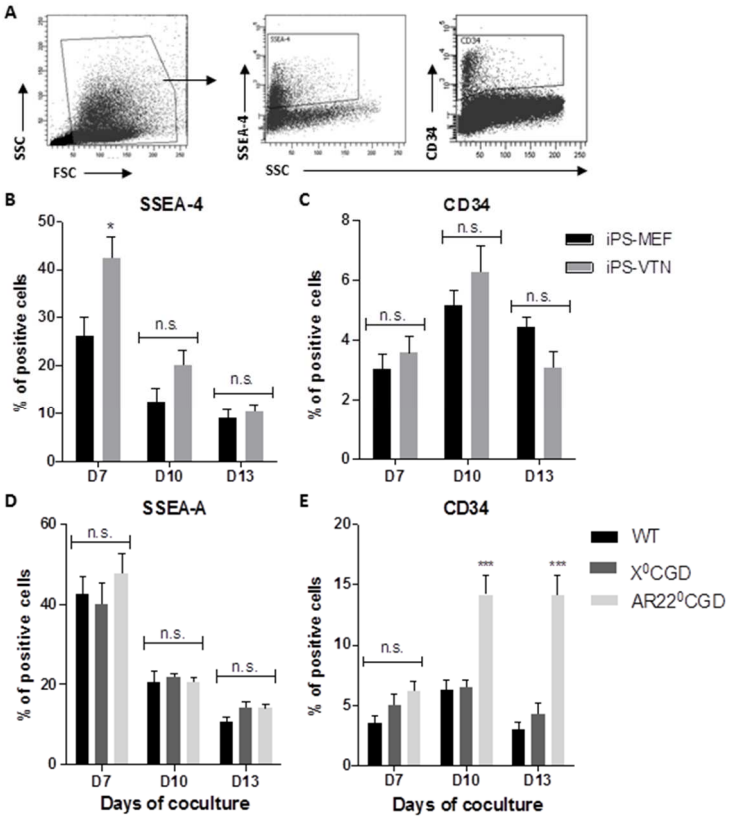

Fig. 1. Kinetic of the hematopoietic differentiation of WT and CGD iPSCs. (A) Plots showing the gating strategy for the analysis by flow cytometry of the expression of SSEA-4 and CD34 markers. **(B)** Histograms showing the percentage of WT cells expressing the membrane pluripotency marker SSEA-4 and **(C)** the hematopoietic marker CD34 at different time point of iPS/OP9 co-culture (days 7, 10 and 13) in MEM medium with ascorbic acid (AA). WT iPS cells were amplified onto irradiated MEFs (iPS-MEF) or in feeder-free condition (iPS-VTN). Data shows mean ± SEM (n=5-6 independent experiments, n.s. non-significant, *p<0.05, unpaired two-tailed Student's *t*-test). Flow cytometry analysis of the percentage of WT and CGD cells expressing the membrane pluripotency marker SSEA-4 **(D)** and the hematopoietic marker CD34 (E) at different time point of iPS/OP9 co-culture (days 7, 10 and 13) in MEM medium with ascorbic acid (AA). Data shows mean ± SEM (n=5-6 independent experiments, n.s. non-significant, *p<0.05, **p<0.01, ***p<0.001, one-way ANOVA significance compared to WT).

Then, we aimed to analyze the impact of NOX deficiency on the kinetic and efficacy of hematopoietic differentiation. The expression of the pluripotency marker SSEA-4 (Fig. 1D) and the hematopoietic marker CD34 (Fig. 1E) was followed between day 7 and day 13 of iPS/OP9 co-culture in WT, X^0CGD and AR22^{0}CGD iPS cells. We observed a progressive disappearance of the expression of the pluripotency marker SSEA-4 between day 7 and day 13 in WT, X^0CGD and AR22^{0}CGD cells with 10-20 % of undifferentiated iPSCs still present in the co-culture at day 13 (Fig. 1D). WT and X^0CGD iPS cell lines showed similar kinetic and efficiency of hematopoietic differentiation, with a peak of about 6.3±2.2% (n=6 independent experiments) and 6.5±1.5% (n=6 independent experiments) CD34$^+$ cells at day 10 respectively, and falling to below 5% at day 13 (Fig. 1E). Unexpectedly, however, the percentage of CD34$^+$ cells differentiated from AR22^{0}CGD iPSCs reached 14.2±3.6% (n=5 independent experiments) by day 10 and remained steady until day 13, representing a 3 to 4-fold increase in differentiated cells on day 13 compared to X^0CGD and WT iPSCs (Fig. 1E). Because different iPS clones from the same donor can show significant heterogeneity in differentiation capacity (50-53), we analyzed another AR22^{0}CGD iPS clone and obtained similar results (Suppl Fig. 1), confirming the specific differentiation behavior of the p22^{phox}-deficient cell lines.

3.2. NADPH oxidase expression in iPSCs and iPSC-derived CD34$^+$ progenitors

In order to determine whether NOX deficiency and presumed changed in redox status could explain the specific behavior of the AR22^{0}CGD cell lines, we first analyzed the NOX phenotype of WT, X^0CGD and AR22^{0}CGD iPSCs (Fig. 2). WT, X^0CGD and AR22^{0}CGD iPSCs expressed mRNA of NOX4 and p22^{phox} but not NOX1 or NOX2 (Fig. 2A); they also expressed DUOX1 mRNA slightly but not NOX3, NOX5 and DUOX2 mRNA (Suppl Fig. 2). Using flow cytometry and western blot analysis and as expected p22^{phox} protein was expressed in WT and X^0CGD but not AR22^{0}CGD iPS cells (Fig. 2B and C). Also as expected from the mRNA results, none of the three iPS cell lines expressed NOX2 protein (Fig. 2B and C). However, despite the presence of NOX4 mRNA in the three iPSC lines, Western blotting revealed no expression of the corresponding protein (Fig. 2C).

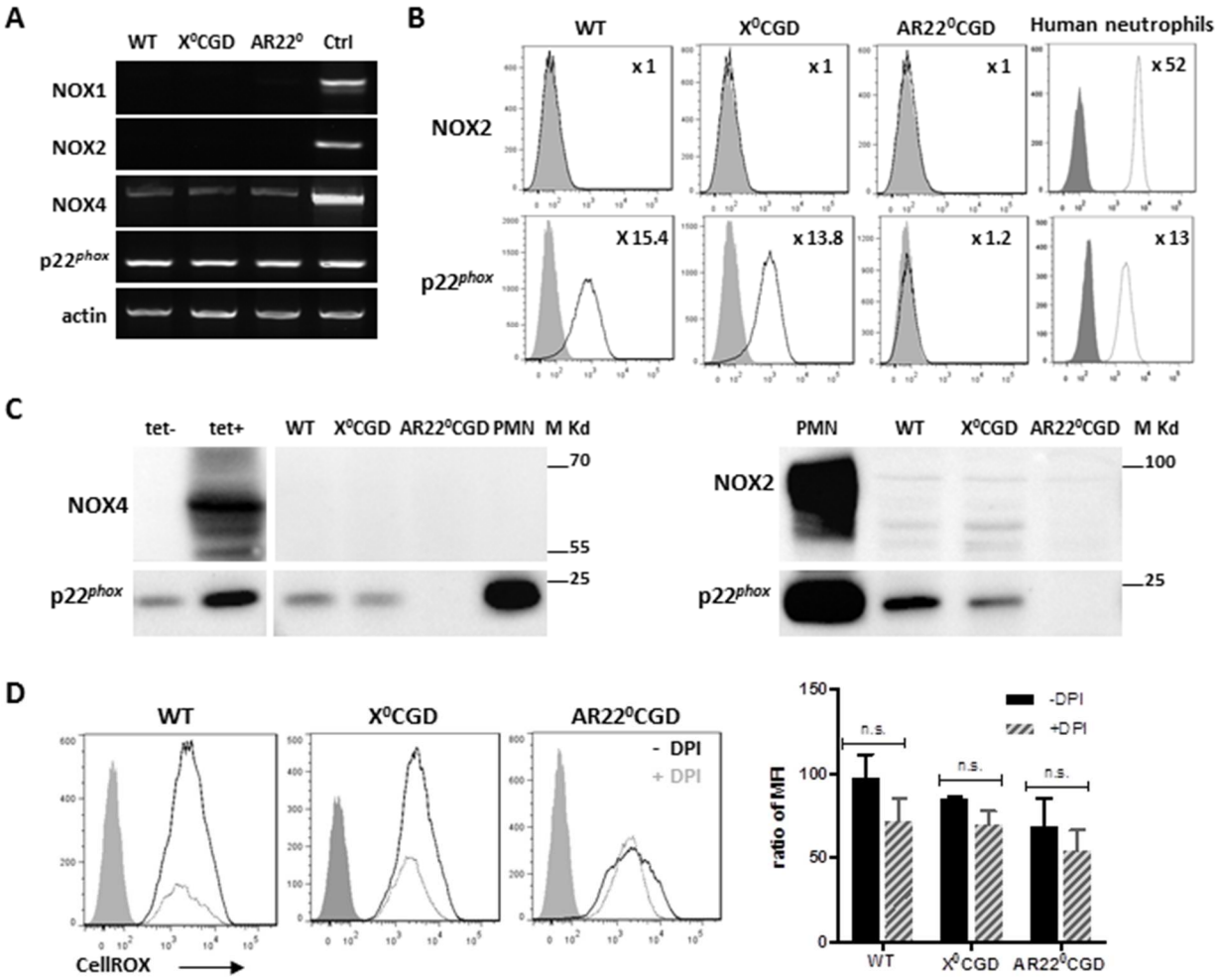

Fig. 2. NADPH oxidase phenotype in iPSCs. (A) Analysis of mRNA expression of NOX1, NOX2, NOX4 and p22^{phox} subunits in WT, X^{0}CGD and AR22^{0}CGD iPSCs was performed by reverse-transcription PCR with primers indicated in Material and Methods (Table 1). β actin was used as positive control of RT-PCR. Positive controls for NOX2, NOX4, and p22^{phox} mRNA expression are done from human lymphocytes (NOX2, p22^{phox}) and tetracycline inducible NOX4 HEK-293 cells [17] **(B)** Expression of NOX2 and p22^{phox} protein subunits by flow cytometry (grey-filled curve = isotype control, black curve = staining). The number indicated the ratio of MFI of the staining *versus* the control. **(C)** Western blotting analysis of NOX2, NOX4 and p22^{phox} protein subunits in soluble extract from WT, X^{0}CGD and AR22^{0}CGD iPSCs (50 µg). Human neutrophils serve as positive control for NOX2 and p22^{phox} expression. Soluble extracts from human neutrophils (PMN 10 µg) and tetracycline-inducible NOX4 HEK-293 cells as controls (tet-, tet+ 5µg) were used as controls [17]. Molecular weight markers are colored protein ladders 10-170 KDa (M, ThermoFisher). **(D)** Intracellular ROS production measured by flow cytometry using the CellROX^{TM} probe (5 µM, 30 min incubation at 37°C) in absence (black curve) or presence of DPI (50 µM, 15 min pre-incubation at 37°C, grey curve) in iPSCs. For negative controls, cells were incubated in absence of CellROX^{TM} (grey-filled curve). Histogram shows the ratio of mean fluorescence intensity (MFI) of cells incubated with CellROX^{TM} to MFI of control cells, bars represent mean ± SEM (n=3-7 independent experiments, one-way ANOVA significance compared to WT at the same day of differentiation, unpaired two-tailed Student's *t*-test compared to the same cell line without DPI). Non-significant (n.s.).

We also analyzed the NOX phenotype of iPSC-derived CD34$^+$ progenitors. As was seen in the iPSCs, differentiating iPSC-derived CD34$^+$ cells did not express NOX1 mRNA (Fig. 3A); nor did they express NOX3, NOX5 and DUOX1 and DUOX2 mRNA (Suppl Fig.2). CD34$^+$ progenitors derived from all iPSC lines expressed NOX4 and p22^{phox} mRNA at each differentiation time, whereas NOX2 mRNA expression started at day 10 for WT increased at day 13 for all cell lines. For AR22^{0}CGD iPSC-derived CD34$^+$ cells, NOX2 mRNA appeared slightly at day 13 (Fig. 3A). We have no explanation for that fact apart that the absence of p22^{phox} protein expression in these cells could have a negative feedback on the expression of NOX2 mRNA.

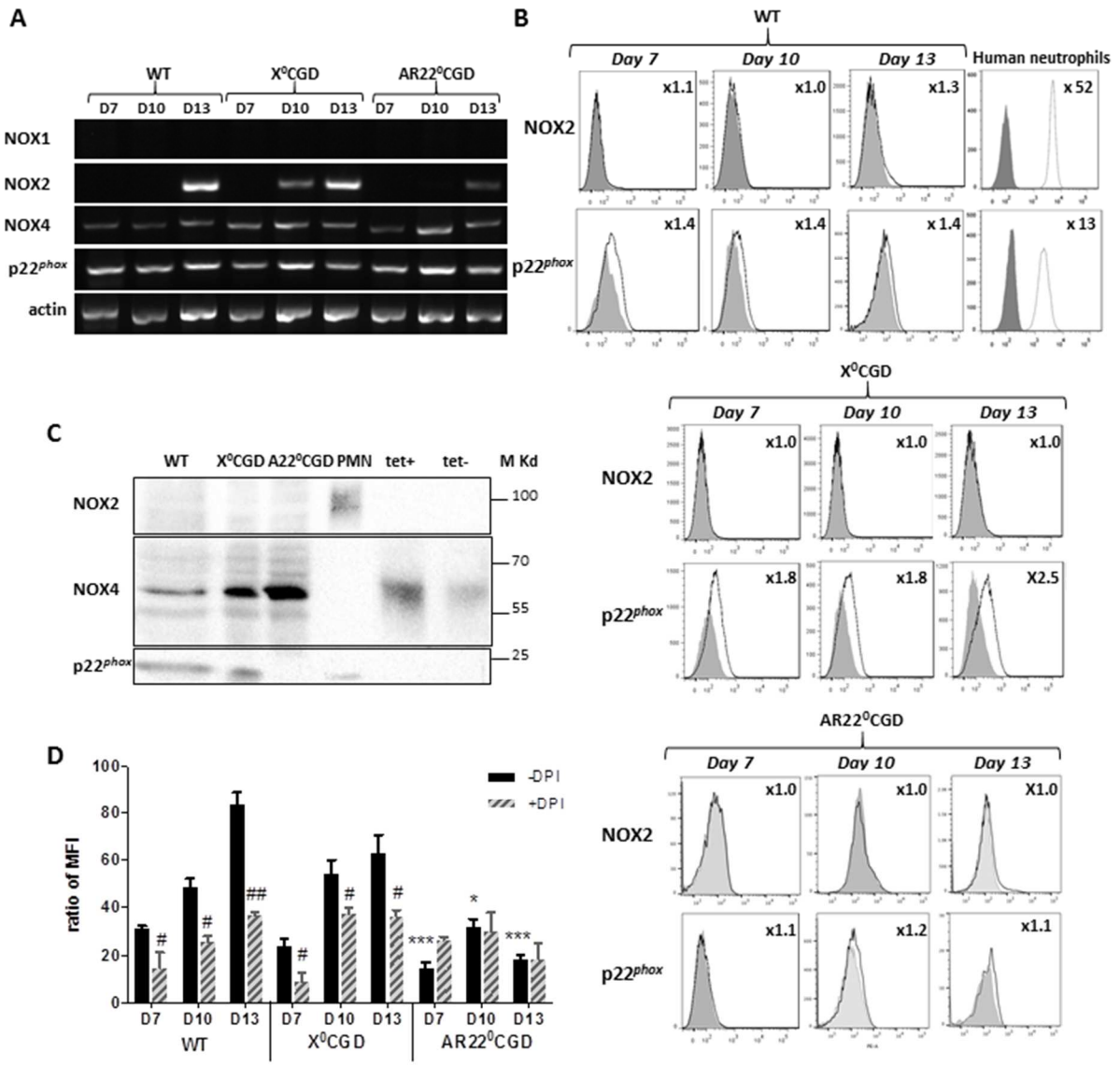

Fig. 3. NADPH oxidase phenotype in iPSC-derived CD34⁺ cells. (A) Analysis of mRNA expression of NOX1, NOX2, NOX4 and p22*phox* subunits at different time of WT, X^{0}CGD and AR22^{0}CGD iPS/OP9 co-cultures was performed by reverse-transcription PCR performed with primers indicated in Material and Methods (Table 1). β actin was used as positive control of RT-PCR. Positive controls for NOX2, NOX4, and p22*phox* mRNA expression are done from human lymphocytes (NOX2, p22*phox*) and tetracycline inducible NOX4 HEK-293 cells [17] **(B)** Expression of NOX2 and p22*phox* protein subunits by flow cytometry (grey-filled curve = isotype control, black curve = staining). The number indicated the ratio of MFI of the staining versus the control. Human neutrophils serve as positive control for NOX2 and p22*phox* expression **(C)** Western blotting analysis of NOX2, NOX4 and p22*phox* protein subunits were performed using 50 µg of soluble extracts from iPSC-derived WT, X^{0}CGD and AR22^{0}CGD CD34⁺ cells. Soluble extracts from human neutrophils (PMN, 2 µg) and tetracycline-inducible NOX4 HEK-293 cells (17) were used as controls (tet-, tet+, 1 µg). Molecular weight markers as colored protein ladders 10-170 KDa (M, ThermoFisher). **(D)** Histogram showing the intracellular ROS production measured by flow cytometry using the CellROX™ probe (5 µM, 30 min incubation at 37°C) in presence or absence of DPI (50 µM, 15 min pre-incubation at 37°C) in iPSC-derived CD34⁺ cells, and expressed as the ratio of MFI of cells incubated with CellROX™ to MFI of control cells not incubated with CellROX™. Data shows mean ± SEM (n=3-7 independent experiments, *p<0.05, **p<0.01, ***p<0.001, one-way ANOVA significance compared to WT at the same day of differentiation; $^{\#}$p<0.05, $^{\#\#}$ p<0.01, unpaired two-tailed Student's *t*-test compared to the same cell line without DPI).

As expected from mRNA results, flow cytometry and Western blot analysis detected $p22^{phox}$ protein only in WT and X^0CGD iPSC-derived $CD34^+$ cells (Fig. 3B and C). However, despite mRNA expression, NOX2 protein was not found in any iPSC-derived $CD34^+$ cells at any time point (Fig. 3B and C). Finally, as expected from mRNA results but in contrast to iPS cells, iPSC-derived $CD34^+$ progenitors expressed NOX4 protein in WT, X^0CGD and $AR22^0$CGD at day 10 of differentiation (Fig. 3C). Thus NOX4 is the unique NOX enzyme expressed in iPSC-derived $CD34^+$ progenitors at early stage of differentiation.

3.3. NADPH oxidase activity in iPSCs and iPSC-derived $CD34^+$ progenitors

We used the fluorogenic probe CellROX™ Deep Red Reagent to evaluate intracellular ROS production. This probe detects several derived oxygen species in addition to hydrogen peroxide, is peroxidase independent, and is photostable (54). NOX-dependent ROS production was determined by measuring CellROX™ fluorescence in the presence and absence of DPI, a NOX (and other flavoenzymes) inhibitor. All types of iPSCs showed similar level of ROS and no significant inhibition by DPI (Fig. 2D), suggesting that iPSCs lack NOX activity, as expected from lack of NOX protein expression in iPSCs. This ROS production is probably due to other ROS production systems as mitochondria.

The pattern of ROS production in $CD34^+$ cells showed two major differences from that of iPSCs. First, intracellular ROS in WT and X^0CGD iPSC-derived $CD34^+$ progenitors was at the same levels and increased similarly from day 7 to 13 of differentiation; in contrast $AR22^0$CGD $CD34^+$ progenitors produced only about half as much ROS as the other two cell lines (Fig. 3D). Secondly, DPI inhibited ROS production by 40-60% in WT and X^0CGD $CD34^+$ progenitors, suggesting this fraction of ROS production was NOX dependent. However, DPI did not inhibit ROS production in $AR22^0$CGD iPSC-derived progenitors; this result was expected, because the absence of $p22^{phox}$ should prevent the activity of the NOX4 protein expressed in these cells. In addition ROS production was obtained without any stimulation as a constitutive production. This is in accordance with the presence of NOX4 in iPSC-derived $CD34^+$ progenitors.

These results suggest that: 1) NOX4/$p22^{phox}$ is responsible for a constitutive ROS production in WT and X^0CGD iPSC-derived-$CD34^+$ cells; 2) NOX4/$p22^{phox}$ produces about half of the ROS in $CD34^+$ cells derived from WT and X^0CGD iPSCs; 3) mitochondrial respiration probably accounts for the low ROS production of $AR22^0$CGD iPSC-derived progenitors; 4) ROS measured in $AR22^0$CGD are NOX independent and are equivalent as the DPI independent ROS production of the WT and X^0CGD iPSC-derived-$CD34^+$ cells .

3.4. Hematopoietic potential of CGD iPSC-derived $CD34^+$ cells

To determine the relationship between the level of ROS production and the hematopoietic ability of the progenitors, we performed an *in vitro* clonogenic colony-forming cell (CFC) assay (Fig. 4). As expected, we observed a similar number of colony-forming units (CFU) arising from WT and X^0CGD iPS/OP9 co-cultures, which increased from day 7 to 13 (Fig. 4A). However only few colonies were obtained from the AR22^{0}CGD iPS/OP9 co-cultures; although the percentage of $CD34^+$ cells present was higher than in WT and X^0CGD iPS/OP9 co-cultures (Fig. 1B). The specific hematopoietic potential of the $CD34^+$ cells was also evaluated by calculating the number of CFU produced from 100,000 $CD34^+$ generated during the co-culture (Fig. 4B).

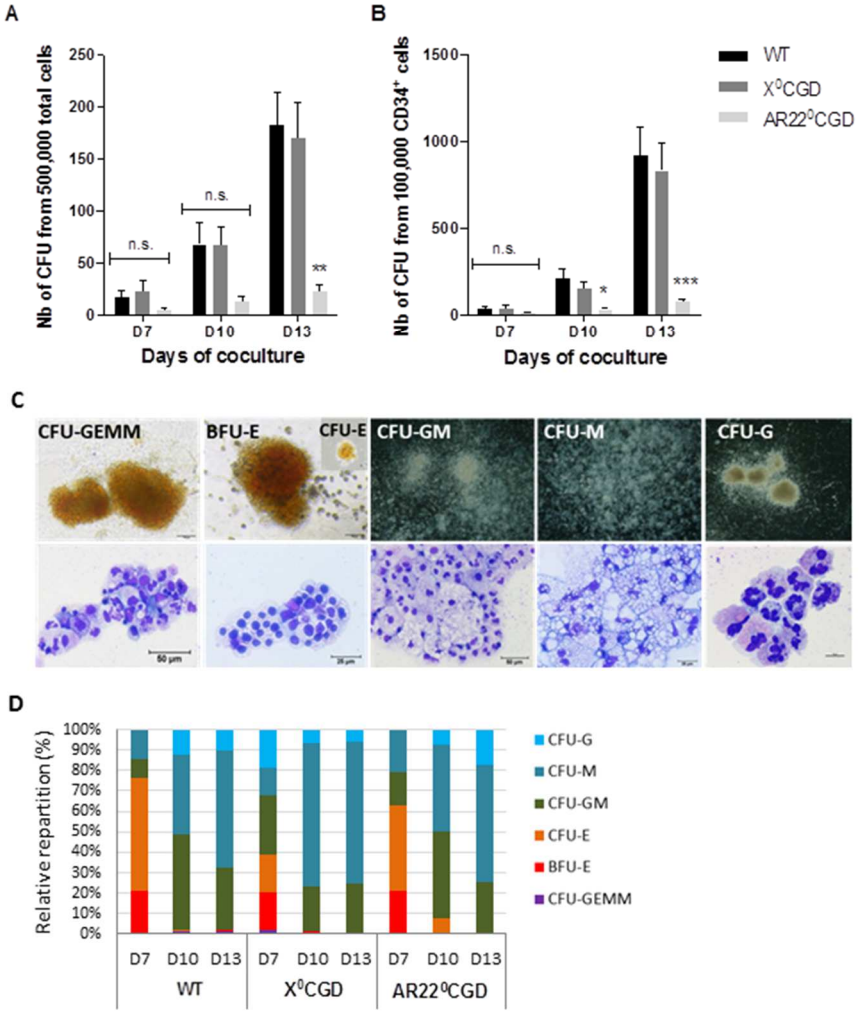

Fig. 4. *In vitro* hematopoietic potential of the CGD iPSC-derived progenitor cells. (A) CFU potential of the cells derived from day 7, 10 and 13 iPS/OP9 co-culture performed into MEM+AA medium. Cells were plated into methylcellulose with hematopoietic cytokines and the number of CFUs counted after 14 days. **(B)** Calculation of the CFU potential considering the percentage of $CD34^+$ cells plated in order to assess the short-term differentiation capabilities of the $CD34^+$ hematopoietic progenitors. For A and B, data shows mean ± SEM (n=3-7 independent experiments, *p<0.05, **p<0.01, ***p<0.001, one-way ANOVA significance compared to WT). **(C)** Representative images for the hematopoietic colonies CFUs obtained after 14 days of culture: CFU-GEMM, BFU-E and CFU-E (magnification x10), CFU-GM, CFU-M and CFU-G (magnification x4) (upper panel) and MGG staining (lower panel, scale bars indicated). **(D)** Relative repartition of the different types of CFUs obtained after 7, 10 and 13 days of WT and CGD iPS/OP9 co-culture in MEM+AA medium. Data shows the mean of n=5 independent experiments.

From these results we confirmed that the hematopoietic potential of the CD34$^+$ progenitors was significantly lower in AR22^{0}CGD than in WT and X^{0}CGD cell lines. The repartition of the different types of colonies, identifiable by their specific morphology and their cell composition (Fig. 4C), was similar in all types of cell lines and varied according to the time of co-culture with more erythroid colonies (BFU-E and CFU-E) at day 7 and a majority of G-, M- or GM-CFUs at day 10 and 13 (Fig. 4D, means ± SD in Table 2).

In conclusion, WT and X^{0}CGD iPSC-derived CD34$^+$ cells displayed an increasing hematopoietic potential with co-culture time while AR22^{0}CGD iPSC-derived CD34$^+$ cells have a constant low hematopoietic potential.

3.5. Phenotypic analysis of the CD34$^+$ progenitors derived from WT, X^{0}CGD and AR22^{0}CGD iPSCs

Finally, we measured the expression of additional markers (CD38, CD45, CD90, CD117, CD133, CXCR4 and CD45RA) via flow cytometry to more fully characterize the phenotype of hematopoietic progenitors produced from the three iPSC lines (Fig. 5). We first observed that from day 7 to 13, the proportion of lineage-committed CD38$^+$ expressing cells remained constant in all three cell lines, while the proportion of cells expressing the pan-hematopoietic marker CD45 was significantly increased by day 13 only in AR22^{0}CGD iPSC-derived CD34$^+$ progenitors (Fig. 5A).

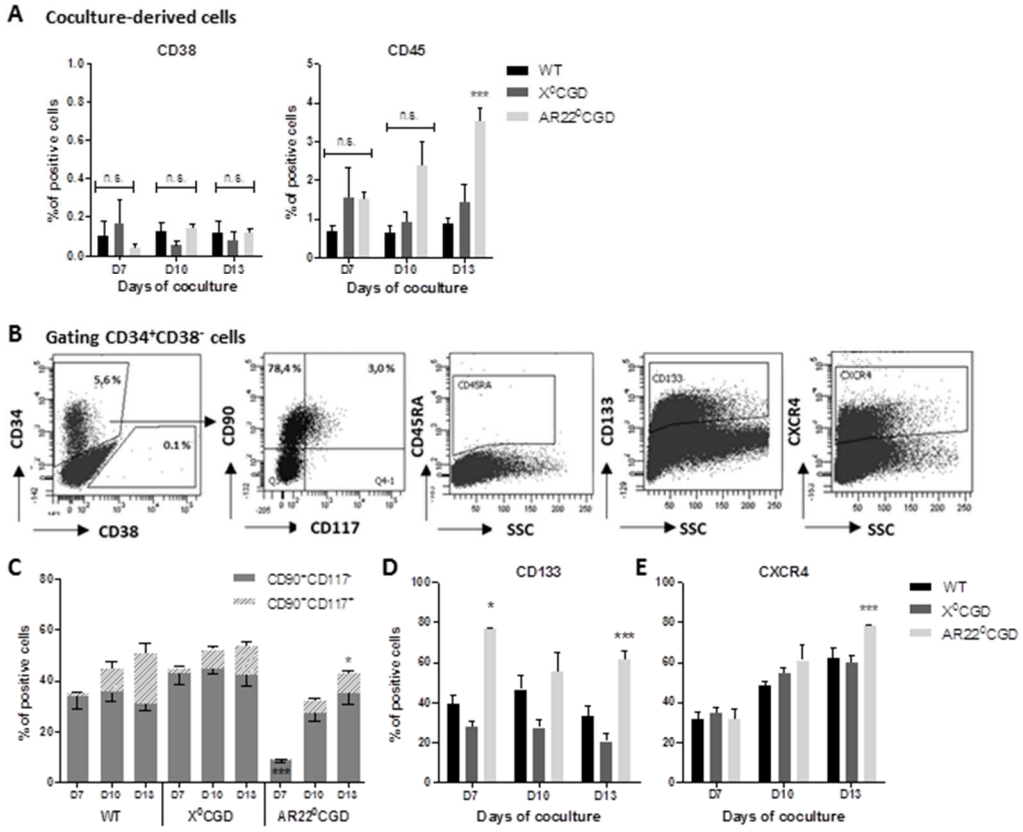

Fig. 5. Phenotypic characterization of iPSC-derived CD34$^+$ hematopoietic progenitors. (A) Flow cytometry analysis of the percentage of cells expressing the hematopoietic markers CD38 and CD45 at different time point of iPS/OP9 co-culture (days 7, 10 and 13). Data shows mean ± SEM (n=5-6 independent experiments, *p<0.05, **p<0.01, ***p<0.001, one-way ANOVA significance compared to WT). **(B)** Representative flow cytometry plots showing the gating of CD34$^+$CD38$^-$ cells and subsequent analysis of CD90/CD117, CR45RA, CD133 and CXCR4 expression. **(C-E)** Histograms showing the percentage of CD34$^+$CD38$^-$ cells expressing the hematopoietic markers CD90 and CD117 **(C)**, CD133 **(D)** and CXCR4 **(E)** at different time points of iPS/OP9 co-culture (days 7, 10 and 13). Data shows mean ± SEM (n=5-6 independent experiments, *p<0.05, **p<0.01, ***p<0.001, one-way ANOVA significance compared to WT).

Then, we analyzed more specifically the phenotype of the CD34$^+$CD38$^-$ population as presented in Fig. 5B. The precise phenotype of HSCs is difficult to determine, but several established markers have been used to enrich for long-term HSCs: Lin$^-$CD34$^+$CD38$^-$CD90$^+$CD45RA$^-$ (55, 56); CD117, the receptor for stem cell growth factor (SCF); and CD133 (57-60). We detected no expression of the CD45RA marker by the CD34$^+$CD38$^-$ progenitors derived from any of the cell lines and at all the time points analyzed. Figure 5C showed that more than 35% of the WT and X^{0}CGD CD34$^+$CD38$^-$ cells expressed the CD90 hematopoietic marker on day 7, with a progressive increase to 50-60% by day 13. These lines also showed a progressive increase of CD90$^+$CD117$^+$ cells. In contrast less than 10% of the AR22^{0}CGD CD34$^+$CD38$^-$ progenitors were CD90$^+$ at day 7, and reached only 40% by day 13, and the proportion of CD117$^+$ cells was also significantly lower at day 13 than the WT and X^{0}CGD cell lines. Surprisingly, the proportion of CD34$^+$CD38$^-$ cells derived from the AR22^{0}CGD iPSCs expressing the more primitive marker CD133 was significantly higher than those derived from WT and X^{0}CGD iPSCs, especially at day 7 of co-culture when the proportion of CD133$^+$ cells in the AR22^{0}CGD line was twice that of the other cell lines (Fig. 5D). Moreover, the expression of the bone marrow homing marker CXCR4 (61) by the CD34$^+$CD38$^-$ progenitors strongly increased during the time-course of co-culture for all types of cell lines (Fig. 5E). The proportion of CXCR4$^+$ cells in the AR22^{0}CGD iPSC-derived CD34$^+$CD38$^-$ cells was significantly higher than the other two lines only at day 13 of differentiation (Fig. 5E).

Taken together, these data demonstrate that day 7 to 13 co-cultures allow the production of various stages of hematopoietic cells including primitive progenitors with a phenotype similar to LT-HSCs (CD34$^+$CD38$^-$CD45RA$^-$CD133$^+$CD90$^+$) (62) but also to more engaged progenitors responsible for the production of hematopoietic colonies in the CFC assay. X^{0}CGD iPSC-derived CD34$^+$CD38$^-$ cells possessed a phenotype similar to the WT iPSCs whatever the time of co-culture, but the phenotype of AR22^{0}CGD iPSC-derived CD34$^+$CD38$^-$ cells was very different than the other two lines.

4. Discussion

Given the accumulating evidence that ROS produced by NADPH oxidases affect the fate of HSCs, we hypothesized that NOX deficiency and resulting lower ROS production could impact

hematopoietic differentiation of CD34$^+$ progenitors produced *in vitro*. We therefore investigated the presence and the role of NOXs during the early stages of *in vitro* hematopoietic differentiation using human iPSC lines deficient in the NOX2 protein (X^{0}CGD) or deficient in activity of NOX1/2/3/4 (AR22^{0}CGD).

We first aimed to improve the iPS cell maintenance of our culture using more defined reagents. In the literature, various methods (feeder cells, Matrigel^R, Vitronectin^R, among others) have produced hematopoietic differentiation of ES/iPSCs. Thus the impact of the iPS culture method on the subsequent differentiation is difficult to evaluate (63). Here, we confirmed that the feeder-free culture of iPSCs using a defined xeno- and serum-free medium does not modify either the kinetics or the efficacy of early hematopoietic differentiation compared to iPSCs cultured on MEFs. The iPS/OP9 co-culture technique is a well-used approach to recapitulate hematopoietic differentiation *in vitro* (64-66). Although not perfect, we thought that this approach was the best way to mimic the interaction of HSCs with stromal cells in the bone marrow niche. We previously used it to produce CD34$^+$ progenitors and to induce their terminal differentiation into mature phagocytic cells (33). We did not notice any difference in terms of kinetics or yield during the production of mature X^{0}CGD and AR22^{0}CGD neutrophils and macrophages compared to WT cells. Focusing on the early stage of hematopoietic differentiation from iPSCs in the present work, we noticed that WT and X^{0}CGD iPSC-derived CD34$^+$ progenitors shared very similar NADPH oxidase activity and ROS production at days 7, 10 and 13 (Figs. 2 and 3). However, we detected no NOX2 expression either mRNA or protein, in iPSCs or in CD34$^+$ cells before day 13; in our hands, NOX2 is only detectable later during the myeloid differentiation of WT iPSC-derived CD34$^+$ cells when the CD45 marker expression increases (unpublished data). The absence of NOX2 expression in iPSCs and its appearance upon neuronal induction was observed by our collaborators using WT and X^{0}CGD iPSCs from the same origin (67), although another study describes a role of NOX2 and NOX4 in the maintenance of pluripotency and in regulation of self-renewal of murine iPSCs cultured on MEFs (68). In any case, we deduce that NOX2 is not the isoform responsible for the NOX activity observed before day 13 of hematopoietic differentiation.

We also did not observe any NOX1, NOX3, NOX5, and DUOX2 mRNA in iPSCs or iPSC-derived CD34$^+$ progenitor cells. DUOX1 mRNA was only slightly expressed in iPSCs. On the other hand, we demonstrated that in WT and X^{0}CGD cell lines, p22^{phox} and NOX4 are expressed in iPSC-derived CD34$^+$ progenitor cells, making NOX4 the only NOX isoform expressed at the early stage of hematopoietic differentiation. It is not surprising that NOX4 is expressed upon hematopoietic induction because NOX4 was shown to drive the differentiation of mESCs into SMC (69) and cardiomyocytes (70), and to regulate the proliferation of neural stem cells (71). NOX1 expression in CD34$^+$ cells seems to be more controversial. We did not find a NOX1 mRNA expression in iPSC-derived CD34$^+$ progenitors, in

agreement with previous works (12, 72), although NOX1 mRNA expression has been reported in healthy and malignant $CD34^+$ cells (15, 20, 73). We do not have an explanation for the discrepancy except that the presence of NOX1 mRNA does guarantee the presence of the corresponding protein. We must also underline that unlike the NOX isoforms, $p22^{phox}$ protein is found in all types of iPSCs except in $AR22^0$ iPSCs. This demonstrates $p22^{phox}$ expression independent from that of NOX enzymes, different from what is observed in phagocytes. We note that during embryonic development $p22^{phox}$ was shown to be expressed independently of NOX isoforms in hemocytoblast (74).

The choice of a specific probe for ROS detection in HSCs is a difficult issue (75). The CellROX™ probe has been widely used within the last 3 years for the quantification of ROS in HSCs (76-78). Using this probe, Rönn *et al*. showed $CD34^+CD45^+$ cells generated *in vitro* from ESCs and iPSCs produced high levels of ROS that induced DNA damage, leading to a decrease of hematopoietic potential and proliferation ability (22). Using the same probe, we measured a progressive elevation of ROS in WT and X^0CGD progenitors until day 13 of hematopoietic differentiation, leading us to conclude that the ROS level is higher in more engaged $CD34^+$ progenitors. However, we did not find any apoptosis or necrosis in our $CD34^+$ cells during the time-course of differentiation before and after sorting (Suppl Fig. 3). Our DPI inhibition results provide good evidence that 50% of the intracellular ROS production in WT and X^0CGD iPSC-derived $CD34^+$ progenitors is NOX-dependent, the remaining was probably produced by mitochondria or ROS-producing NOX-independent enzymes. This result is also in accordance with previous evaluations of NOX-dependent ROS production in HSCs (12, 15). The phenotype of $AR22^0$CGD iPSC-derived $CD34^+$ progenitors was strikingly different from that of WT and X^0CGD iPSC-derived $CD34^+$ progenitors in that the absence of $p22^{phox}$ protein expression abrogates the NADPH oxidase activity despite expression of NOX4 protein. Because NOX4 is the only NOX isoform expressed in $CD34^+$ cells induced from iPSCs in these cell lines, and because the pattern of $p22^{phox}$ expression matches the pattern of NOX-dependent ROS production, we ascribe the observed NOX-derived ROS production to NOX4. In addition ROS production in WT and X^0CGD iPSC-derived $CD34^+$ progenitors was constitutive underlying the presence of NOX4 expression in these cells in the early stage of hematopoietic differentiation.

The $AR22^0$CGD cell type showed a 3-fold higher production of $CD34^+$ progenitors at day 13 compared to the production of WT and X^0CGD iPSC-derived $CD34^+$ progenitors; clone-to-clone variability was tested (data not shown) but does not explain our results. This suggests that $AR22^0$CGD accumulates $CD34^+$ progenitors delayed in their maturation by the absence of NOX4 activity. Another study showed that culture of human $CD34^+$ cells with DPI or N-acetyl-cysteine inhibits the differentiation process and the colony growth while increasing the number of $CD34^+$ cells (72) thus supporting our observation with the $AR22^0$CGD cell line.

It is well established that increased levels of ROS in HSCs are responsible for the shift from quiescence to cycling proliferation and in consequence for the loss of stemness and HSC function (3, 6, 8, 18), yet excess ROS can also induce senescence and apoptosis (11, 22). The progressive increase of intracellular ROS level in WT and X^0CGD over the course of differentiation was associated with an increase of their hematopoietic progenitor capacity. The kinetics and the types of CFC obtained during the *in vitro* hematopoietic differentiation of all types of iPSCs, reproduces the sequence of events observed during human embryonic development with erythroid progenitors appearing earlier than myeloid progenitors (65, 79-81). Erythroid colonies are more sensitive to ROS (22), which probably explains why we observed them mainly at day 7 when iPSC-derived $CD34^+$ progenitors of all types produce the lowest level of ROS. Although the proportion of the different types of CFU during the time-course of differentiation is identical for all 3 types of $CD34^+$ progenitors, the absolute number of CFU was drastically lower in the $AR22^0$CGD iPSC-derived $CD34^+$ progenitors compared to the WT and X^0CGD iPSC-derived $CD34^+$ progenitors. NOX4 activity seems to be involved in the control of the $CD34^+$ progenitor maturation that is linked to their hematopoietic potential. Fan *et al*. also demonstrated that ROS mediate the differentiation process *in vitro* in HSCs (72). All the cell lines were $CD45RA^-$ as primitive progenitors. In addition, we found that the hematopoietic differentiation of $p22^{phox}$-deficient iPS cell line produced more $CD34^+CD38^-$ progenitors expressing the primitive marker CD133, but less $CD90^+$ cells at day 7 compared to the WT and X^0CGD iPSC-derived $CD34^+$ progenitors. According to the literature, the phenotype of the progenitors during hematopoiesis can be described as primitive ($CD34^+133^+90^+$), early ($CD34^+133^+90^-$) and committed ($CD34^+133^-$) progenitors (55, 62). However the primitive CD133 marker (82, 83) seems to be acquired before the CD90 marker with a majority of $CD133^+CD90^-$ progenitors produced at day 7 and a progressive accumulation of $CD133^+CD90^+$ progenitors during the *in vitro* induced hematopoietic differentiation. Thus these latter results support the idea that the absence of NOX4-dependent ROS production in the $AR22^0$CGD iPSC-derived $CD34^+$ progenitors is responsible for a retardation of maturation explaining the low hematopoietic progenitor potential in these cells. We also noticed that at D13 of differentiation, CD117 marker was less expressed in $AR22^0$CGD iPSC-derived $CD34^+CD38^-$ progenitors than in WT and X^0CGD iPSC-derived $CD34^+CD38^-$ progenitors suggesting again a delayed maturation although the hierarchy of hematopoietic maturation remains difficult to translate in the context of *in vitro* differentiation. Interestingly, CXCR4 expression was higher in $AR22^0$CGD iPSC-derived $CD34^+CD38^-$ progenitors although we can't explain this phenomenon. This homing marker is generally highly expressed in HSCs and is essential for bone marrow engraftment after transplantation (84).

Humanized mouse obtained after engraftment of HSCs in immunodeficient mice could represent pertinent animal models to mimic as close as possible human genetic pathologies like CGD (85). However, human iPSC-derived hematopoietic cells display a phenotype different from *in vivo*

differentiated hematopoietic stem cells that could explain their lower efficient engraftment in immunodeficient mice (27). Until 2013, only two teams succeeded to obtain a three lineages reconstitution from hiPSCs through the formation of teratoma in mice (86, 87). We suspect that the low oxygen environment of the tumor may have contributed to the development of $CD34^+$ cells with a low redox status that could explain a higher ability to engraft. In addition, a lot of efforts are actually made in order to maintain or restore the stemness of HSPCs by the use of NOXs inhibitors, antioxidants molecules and hypoxic culture, alone or in combination (22, 72, 88-91). Indeed, one limit of the hematopoietic differentiation protocol used in this study is that experiments were conducted under 21% oxygen, and not in hypoxia conditions like HSCs located in a hypoxia niche inside the bone marrow. Thus, considering the most probable role of NOX4 as an oxygen sensor in WT and X^0CGD iPSC-derived $CD34^+$ progenitors, normoxia condition could have induced abnormal activation of NOX4 in these 2 types of cells. This is not the case in the $AR22^0$CGD iPSC-derived $CD34^+$ progenitors where the absence of $p22^{phox}$ leads to the absence of NOX4 activity. Thus $AR22^0$CGD iPSC-derived $CD34^+$ progenitors with their specific phenotype related to a low redox status, could be the best cell line for a successful engraftment in immunodeficient mice to model CGD. In addition very recently it was demonstrated that beside the redox status of the hematopoietic progenitors, transduction of specific transcription factors in human ES/iPS are also very important to promote engraftment and multi-lineage differentiation (92, 93). This could be another way to increase the efficiency of engraftment in immunodeficient mice in order to generate pathological animal models.

This study brings additional evidences that NOX4 is the main ROS-producing NOX isoform in $CD34^+CD38^-$ progenitors during the early stages of *in vitro* hematopoietic differentiation and that NADPH oxidase deficiency (in $p22^{phox}$ deficient cells) is associated with low intracellular ROS level, accumulation of primitive $CD34^+$ progenitors with a delayed maturation related to a low functional hematopoietic progenitor ability. However, in later stage of hematopoiesis differentiation other ROS-producing systems probably take over because $AR22^0$CGD patients don't have any defect regarding mature hematopoietic cells in the peripheral blood. In addition, an important role of NOX2 cannot be excluded at later stages of hematopoietic differentiation than analyzed here (94). Thus, more studies should be performed in order to investigate the role of NOX2 and other ROS-producing systems in later stages of hematopoietic differentiation.

Acknowledgments

A warm thank to Prof Ulla Knaus from the Dublin University, Ireland, for the generous gift of NOX4 antibodies and to Prof Susan Smith from Kennesaw University, USA, for editing the manuscript. We also thank Prof Karl Heinz Krause and Dr Vincent Jaquet for the gift of NOX4 inducible HEK-293 cells. We thank Thibaut Kalitynski for his help in molecular biology experiments. Many thanks to Prof Susan Smith and Prof Franck Fieschi for their critical review of the manuscript.

Funding supports

MJS is grateful for supports from the University Grenoble Alpes (UGA) (AGIR program 2014); the Faculty of Medicine and the Pole Recherche, University Hospital Grenoble Alpes (CHUGA), Interreg France-Suisse (Programme de Cooperation Territoriale Europeenne, Fond Europeen de Developpement Regional (FEDER), 2017–2019). This work was also supported by the Delegation for Clinical Research and Innovations (DRCI, Rementips project 2014).

Disclosure statement

The authors declare that they have no conflict of interests.

Table 1

List of primers used for PCR amplification

mRNA	Sequences	Amplicon size
NOX1	5'- GTACAAATTCCAGTGTGCAGACCAC - 3'	397 bp
	5'- CAGACTGGAATATCGGTGACAGCA - 3'	
NOX2	5'- CCTCTGCCACCATGGGGAAC - 3'	296 bp
	5'- GTCCAGTTGTCTTCGAACTCTTG - 3'	
NOX3	5'- GGATCGGAGTCACTCCCTTCGCTG - 3'	458 bp
	5' ATGAACACCTCTGGGGTCAGCTGA - 3'	
NOX4	5'- TCGCCAACGAAGGGGTTAAA - 3'	594 bp
	5'- GCAACGTCAGCAGCATGTAG - 3'	
NOX5	5' - TTATGGGCTACGTGGTAGTGGG - 3	150 bp
	5' - GAACCGTGTACCCAGCCAAT - 3'	
DUOX1	5' - GCAGGACATCAACCCTGCACTCTC - 3'	672 bp
	5' - CTGCCATCTACCACACGGATCTGC - 3'	
DUOX2	5' - CCGGCAATCATCATATGGAGGT - 3'	545 bp
	5' – TTGGATGATGTCAGCCAGCC - 3'	
p22^{phox}	5'- CAGTGTCCCAGCCGGGTTCGTGTC -3'	351 bp
	5'- GATGGTGGCCAGCAGGAAGC -3'	
β-actin	5'- ATCTGGCACCACACCTTCTACAATGAGCTGCG -3'	838 bp
	5'- CGTCATACTCCTGCTTGCTGATCCACATCT -3'	

Table 2

Repartition of the types of CFUs generated from the iPSC-derived $CD34^+$ hematopoietic progenitors. Data shows mean ± SD (n=5-6 independent experiments).

iPS cell line	Day of coculture	CFU-GEMM	BFU-E	CFU-E	CFU-GM	CFU-M	CFU-G
WT	D7	0 (0)	3 (5)	8 (14)	1 (1)	2 (4)	0 (0)
	D10	1 (1)	0 (0)	1 (1)	42 (32)	36 (14)	11 (7)
	D13	2 (2)	1 (2)	0 (0)	51 (44)	97 (36)	18 (8)
X0CGD	D7	0 (1)	3 (4)	3 (5)	5 (5)	2 (3)	3 (4)
	D10	1 (1)	1 (1)	0 (0)	18 (22)	57 (61)	6 (6)
	D13	0 (1)	0 (0)	0 (0)	57 (45)	165 (106)	14 (11)
AR220CGD	D7	0 (0)	1 (1)	2 (2)	1 (1)	1 (1)	0 (0)
	D10	0 (0)	0 (0)	1 (1)	5 (3)	5 (9)	1 (2)
	D13	0 (0)	0 (0)	0 (0)	5 (5)	12 (8)	4 (4)

Supplementary Table 1

Identification of the markers used in this study

Name	Protein	Marker
SSEA4	Stage-specific Embryonic Antigen-4	Embryonic Stem Cell (pluripotency marker)
CD34	Transmembrane phosphoglycoprotein	Early hematopoietic and vascular-associated cell and tissue
CD45	protein tyrosine phosphatase regulating src-family kinases	Hematopoietic cells, leukocytes
CD45RA	Isoform of CD45	Naïve T lymphocytes, memory marker
CD38	Ecto-enzyme, ADP-ribosyl cyclase and ADPRc-hydrolase activities	Late hematopoietic stem cells, lymphocytes
CD117	Proto-oncogene c-Kit, tyrosine-protein kinase Kit	Hematopoietic stem cells, Multipotent progenitors, Common myeloid progenitors
CD90	Thy-1, GPI-anchored protein	Thymocytes, early hematopoietic stem cells, nervous and lymphoid tissues
CD133	prominin-1, transmembrane glycoprotein	Hematopoietic stem cells**,** Endothelial progenitors stem cells
CXCR4	C-X-C chemokine receptor type 4, fusin, CD184, α-chemokine receptor specific for stromal-derived-factor-1	Important for hematopoietic stem cells homing and quiescence

CD means cluster of differentiation

Figure Legends

Figure 1. Kinetic of the hematopoietic differentiation of WT and CGD iPSCs. (A) Plots showing the gating strategy for the analysis by flow cytometry of the expression of SSEA-4 and CD34 markers. **(B)** Histograms showing the percentage of WT cells expressing the membrane pluripotency marker SSEA-4 and **(C)** the hematopoietic marker CD34 at different time point of iPS/OP9 co-culture (days 7, 10 and 13) in MEM medium with ascorbic acid (AA). WT iPS cells were amplified onto irradiated MEFs (iPS-MEF) or in feeder-free condition (iPS-VTN). Data shows mean ± SEM (n=5-6 independent experiments, n.s. non significant, *p<0.05, unpaired two-tailed Student's *t*-test). Flow cytometry analysis of the percentage of WT and CGD cells expressing the membrane pluripotency marker SSEA-4 **(D)** and the hematopoietic marker CD34 (E) at different time point of iPS/OP9 co-culture (days 7, 10 and 13) in MEM medium with ascorbic acid (AA). Data shows mean ± SEM (n=5-6 independent experiments, n.s. non significant, *p<0.05, **p<0.01, ***p<0.001, one-way ANOVA significance compared to WT).

Figure 2. NADPH oxidase phenotype in iPSCs. (A) Analysis of mRNA expression of NOX1, NOX2, NOX4 and $p22^{phox}$ subunits in WT, X^0CGD and $AR22^0$CGD iPSCs was performed by reverse-transcription PCR with primers indicated in Material and Methods (Table 1). β actin was used as positive control of RT-PCR. Positive controls for NOX2, NOX4, and p22phox mRNA expression are done from human lymphocytes (NOX2, $p22^{phox}$) and tetracycline inducible NOX4 HEK-293 cells [17] **(B)** Expression of NOX2 and $p22^{phox}$ protein subunits by flow cytometry (grey-filled curve = isotype control, black curve = staining). The number indicated the ratio of MFI of the staining *versus* the control. **(C)** Western blotting analysis of NOX2, NOX4 and $p22^{phox}$ protein subunits in soluble extract from WT, X^0CGD and $AR22^0$CGD iPSCs (50 µg). Human neutrophils serve as positive control for NOX2 and $p22^{phox}$ expression. Soluble extracts from human neutrophils (PMN 10 µg) and tetracycline-inducible NOX4 HEK-293 cells as controls (tet-, tet+ 5µg) were used as controls [17]. Molecular weight markers are colored protein ladders 10-170 KDa (M, ThermoFisher). **(D)** Intracellular ROS production measured by flow cytometry using the CellROX™ probe (5 µM, 30 min incubation at 37°C) in absence (black curve) or presence of DPI (50 µM, 15 min pre-incubation at 37°C, grey curve) in iPSCs. For negative controls, cells were incubated in absence of CellROX™ (grey-filled curve). Histogram shows the ratio of mean fluorescence intensity (MFI) of cells incubated with CellROX™ to MFI of control cells, bars represent mean ± SEM (n=3-7 independent experiments, one-way ANOVA significance compared to WT at the same day of differentiation, unpaired two-tailed Student's *t*-test compared to the same cell line without DPI). Non significant (n.s.).

Figure 3. NADPH oxidase phenotype in iPSC-derived CD34$^+$ cells. (A) Analysis of mRNA expression of NOX1, NOX2, NOX4 and p22^{phox} subunits at different time of WT, X^{0}CGD and AR22^{0}CGD iPS/OP9 co-cultures was performed by reverse-transcription PCR performed with primers indicated in Material and Methods (Table 1). β actin was used as positive control of RT-PCR. Positive controls for NOX2, NOX4, and p22^{phox} mRNA expression are done from human lymphocytes (NOX2, p22^{phox}) and tetracycline inducible NOX4 HEK-293 cells [17] **(B)** Expression of NOX2 and p22^{phox} protein subunits by flow cytometry (grey-filled curve = isotype control, black curve = staining). The number indicated the ratio of MFI of the staining versus the control. Human neutrophils serve as positive control for NOX2 and p22^{phox} expression **(C)** Western blotting analysis of NOX2, NOX4 and p22^{phox} protein subunits were performed using 50 µg of soluble extracts from iPSC-derived WT, X^{0}CGD and AR22^0 CD34$^+$ cells. Soluble extracts from human neutrophils (PMN, 2 µg) and tetracycline-inducible NOX4 HEK-293 cells (17) were used as controls (tet-, tet+, 1 µg). Molecular weight markers as colored protein ladders 10-170 KDa (M, ThermoFisher). **(D)** Histogram showing the intracellular ROS production measured by flow cytometry using the CellROX^{TM} probe (5 µM, 30 min incubation at 37°C) in presence or absence of DPI (50 µM, 15 min pre-incubation at 37°C) in iPSC-derived CD34$^+$ cells, and expressed as the ratio of MFI of cells incubated with CellROX^{TM} to MFI of control cells not incubated with CellROX^{TM}. Data shows mean ± SEM (n=3-7 independent experiments, *p<0.05, **p<0.01, ***p<0.001, one-way ANOVA significance compared to WT at the same day of differentiation; $^{\#}$p<0.05, $^{\#\#}$p<0.01, unpaired two-tailed Student's *t*-test compared to the same cell line without DPI).

Figure 4. *In vitro* hematopoietic potential of the CGD iPSC-derived progenitor cells. (A) CFU potential of the cells derived from day 7, 10 and 13 iPS/OP9 co-culture performed into MEM+AA medium. Cells were plated into methylcellulose with hematopoietic cytokines and the number of CFUs counted after 14 days. **(B)** Calculation of the CFU potential considering the percentage of CD34$^+$ cells plated in order to assess the short-term differentiation capabilities of the CD34$^+$ hematopoietic progenitors. For A and B, data shows mean ± SEM (n=3-7 independent experiments, *p<0.05, **p<0.01, ***p<0.001, one-way ANOVA significance compared to WT). **(C)** Representative images for the hematopoietic colonies CFUs obtained after 14 days of culture: CFU-GEMM, BFU-E and CFU-E (magnification x10), CFU-GM, CFU-M and CFU-G (magnification x4) (upper panel) and MGG staining (lower panel, scale bars indicated). **(D)** Relative repartition of the different types of CFUs obtained after 7, 10 and 13 days of WT and CGD iPS/OP9 co-culture in MEM+AA medium. Data shows the mean of n=5 independent experiments.

Figure 5. Phenotypic characterization of iPSC-derived $CD34^+$ hematopoietic progenitors. (A) Flow cytometry analysis of the percentage of cells expressing the hematopoietic markers CD38 and CD45 at different time point of iPS/OP9 co-culture (days 7, 10 and 13). Data shows mean ± SEM (n=5-6 independent experiments, *p<0.05, **p<0.01, ***p<0.001, one-way ANOVA significance compared to WT). **(B)** Representative flow cytometry plots showing the gating of $CD34^+CD38^-$ cells and subsequent analysis of CD90/CD117, CR45RA, CD133 and CXCR4 expression. **(C-E)** Histograms showing the percentage of $CD34^+CD38^-$ cells expressing the hematopoietic markers CD90 and CD117 **(C)**, CD133 **(D)** and CXCR4 **(E)** at different time points of iPS/OP9 co-culture (days 7, 10 and 13). Data shows mean ± SEM (n=5-6 independent experiments, *p<0.05, **p<0.01, ***p<0.001, one-way ANOVA significance compared to WT).

Supplementary Figure 1. Kinetic of the hematopoietic differentiation of $AR22^0CGD$ iPSCs. Histogram showing the percentage of two distinct clones of $AR22^0CGD$ (C2 and C3) cells expressing the hematopoietic marker CD34 at different time point of iPS/OP9 coculture (days 7, 10 and 13) in MEM medium with ascorbic acid (AA). $AR22^0CGD$ iPS cells were amplified onto irradiated MEFs (iPS-MEF). Data shows mean ± SEM (n=5-6 independent experiments).

Supplementary Figure 2. NOX3, NOX5, DUOX1 and DUOX2 mRNA expression in iPSCs and iPSC-derived $CD34^+$ cells. Analysis of mRNA expression of NOX3, NOX5, DUOX1 and DUOX2 in WT, X^0CGD and $AR22^0CGD$ iPSCs (A) and in iPSC derived WT, X^0CGD and $AR22^0CGD$ $CD34^+$ progenitors was performed by reverse-transcription PCR with primers indicated in Material and Methods (Table 1). β actin was used as positive control of RT-PCR. Positive controls for NOX3, NOX5, DUOX1 and DUOX2 mRNA expression are done from NOX3 PLB-985 cells, Caco2 cells (NOX5 and DUOX2) and human lymphocytes (DUOX1).

Supplementary Figure 3. Apoptosis and necrosis analysis in WT (A), X^0CGD (B) and $AR22^0CGD$ (C) $CD34^+$ progenitors. 1.10^5 iPSCs derived WT, X^0CGD and $AR22^0CGD$ $CD34^+$ progenitors before and after $CD34^+$ sorting with CD34 magnetic beads (Miltenyi Biotec), were incubated with FITC-Annexin V and propidium iodide for 15 min at room temperature in the dark according to the manufacturer's instructions (FITC Annexin V Apoptosis Detection Kit, BD Biosciences) and then analyzed using a FACS Canto II (BD Biosciences). Data were collected and analyzed with the FACS DIVA software (BD Biosciences) and FlowJo software (Tree Star).

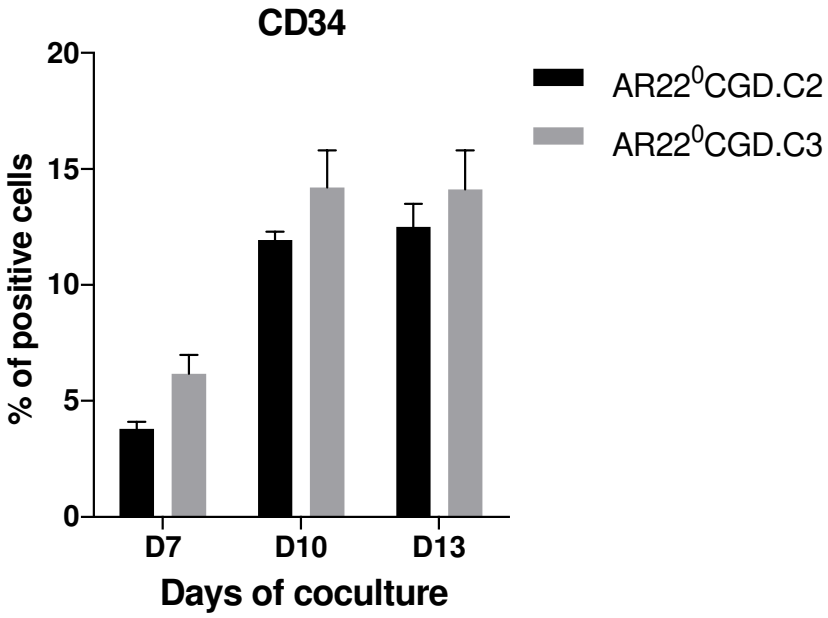

Supplementary Figure 1

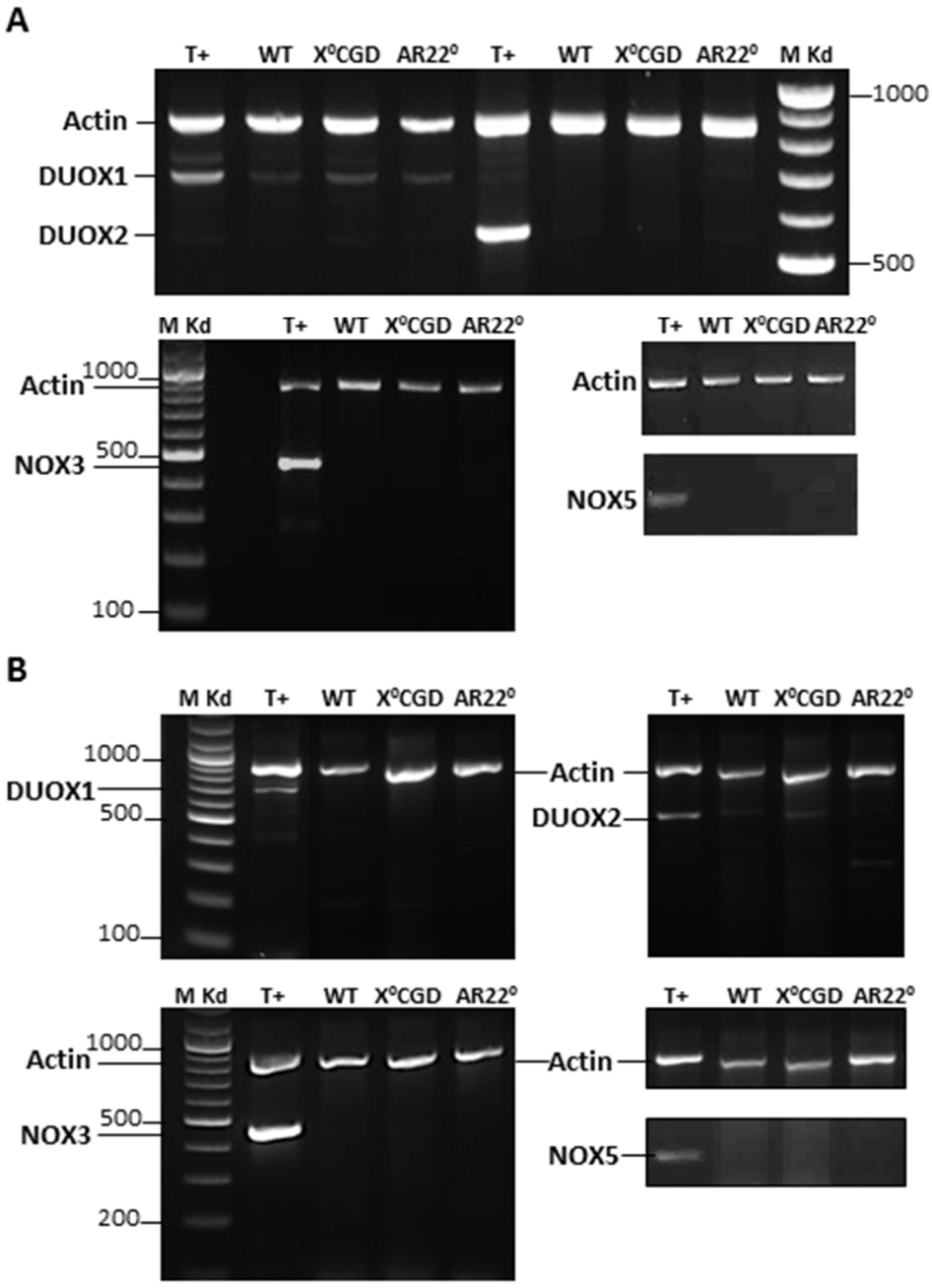

Supplementary Figure 2

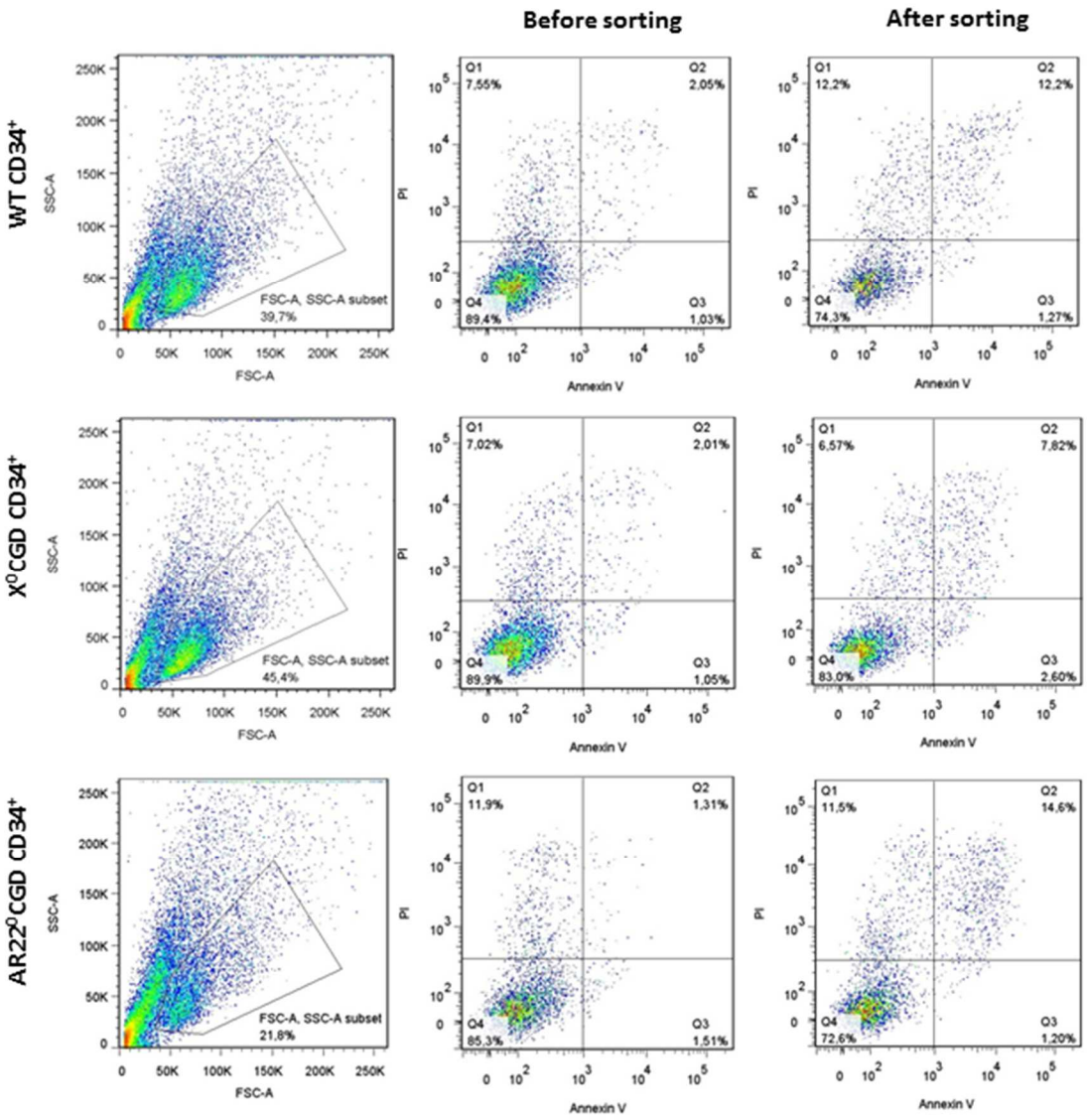

Supplementary Figure 3

References

1. Bigarella CL, Liang R, Ghaffari S. Stem cells and the impact of ROS signaling. Development. 2014;141(22):4206-18.
2. Haneline LS. Redox regulation of stem and progenitor cells. Antioxid Redox Signal. 2008;10(11):1849-52.
3. Ushio-Fukai M, Rehman J. Redox and Metabolic Regulation of Stem/Progenitor Cells and Their Niche. Antioxid Redox Sign. 2014;21(11):1587-90.
4. Brieger K, Schiavone S, Miller FJ, Krause KH. Reactive oxygen species: from health to disease. Swiss Med Wkly. 2012;142.
5. Liang R, Ghaffari S. Stem Cells, Redox Signaling, and Stem Cell Aging. Antioxid Redox Sign. 2014;20(12):1902-16.
6. Ludin A, Gur-Cohen S, Golan K, Kaufmann KB, Itkin T, Medaglia C, et al. Reactive Oxygen Species Regulate Hematopoietic Stem Cell Self-Renewal, Migration and Development, As Well As Their Bone Marrow Microenvironment. Antioxid Redox Sign. 2014;21(11):1605-19.
7. Roy IM, Biswas A, Verfaillie C, Khurana S. Energy Producing Metabolic Pathways in Functional Regulation of the Hematopoietic Stem Cells. Iubmb Life. 2018;70(7):612-24.
8. Piccoli C, Agriesti F, Scrima R, Falzetti F, Di Ianni M, Capitanio N. To breathe or not to breathe: the haematopoietic stem/progenitor cells dilemma. Brit J Pharmacol. 2013;169(8):1652-71.
9. Hu M, Zeng H, Chen S, Xu Y, Wang S, Tang Y, et al. SRC-3 is involved in maintaining hematopoietic stem cell quiescence by regulation of mitochondrial metabolism in mice. Blood. 2018;132(9):911-23.
10. Pervaiz S, Taneja R, Ghaffari S. Oxidative stress regulation of stem and progenitor cells. Antioxid Redox Signal. 2009;11(11):2777-89.
11. Porto ML, Rodrigues BP, Menezes TN, Ceschim SL, Casarini DE, Gava AL, et al. Reactive oxygen species contribute to dysfunction of bone marrow hematopoietic stem cells in aged C57BL/6 J mice. J Biomed Sci. 2015;22:97.
12. Piccoli C, Ria R, Scrima R, Cela O, D'Aprile A, Boffoli D, et al. Characterization of mitochondrial and extra-mitochondrial oxygen consuming reactions in human hematopoietic stem cells. Novel evidence of the occurrence of NAD(P)H oxidase activity. J Biol Chem. 2005;280(28):26467-76.
13. Bedard K, Krause KH. The NOX family of ROS-generating NADPH oxidases: physiology and pathophysiology. Physiol Rev. 2007;87(1):245-313.
14. O'Neill S, Brault J, Stasia MJ, Knaus UG. Genetic disorders coupled to ROS deficiency. Redox Biol. 2015;6:135-56.
15. Piccoli C, D'Aprile A, Ripoli M, Scrima R, Lecce L, Boffoli D, et al. Bone-marrow derived hematopoietic stem/progenitor cells express multiple isoforms of NADPH oxidase and produce constitutively reactive oxygen species. Biochem Biophys Res Commun. 2007;353(4):965-72.
16. Guo SH, Chen XP. The human Nox4: gene, structure, physiological function and pathological significance. J Drug Target. 2015;23(10):888-96.
17. Serrander L, Cartier L, Bedard K, Banfi B, Lardy B, Plastre O, et al. NOX4 activity is determined by mRNA levels and reveals a unique pattern of ROS generation. Biochem J. 2007;406:105-14.
18. Urao N, Ushio-Fukai M. Redox regulation of stem/progenitor cells and bone marrow niche. Free Radical Bio Med. 2013;54:26-39.
19. Song SH, Kim K, Park JJ, Min KH, Suh W. Reactive oxygen species regulate the quiescence of CD34-positive cells derived from human embryonic stem cells. Cardiovasc Res. 2014;103(1):147-55.
20. Guida M, Maraldi T, Beretti F, Follo MY, Manzoli L, De Pol A. Nuclear Nox4-Derived Reactive Oxygen Species in Myelodysplastic Syndromes. Biomed Res Int. 2014.
21. Hole PS, Pearn L, Tonks AJ, James PE, Burnett AK, Darley RL, et al. Ras-induced reactive oxygen species promote growth factor-independent proliferation in human CD34(+) hematopoietic progenitor cells. Blood. 2010;115(6):1238-46.

22. Ronn RE, Guibentif C, Saxena S, Woods NB. Reactive Oxygen Species Impair the Function of CD90(+) Hematopoietic Progenitors Generated from Human Pluripotent Stem Cells. Stem Cells. 2017;35(1):197-206.
23. Dolatshad H, Tatwavedi D, Ahmed D, Tegethoff JF, Boultwood J, Pellagatti A. Application of induced pluripotent stem cell technology for the investigation of hematological disorders. Adv Biol Regul. 2019;71:19-33.
24. Hamazaki T, El Rouby N, Fredette NC, Santostefano KE, Terada N. Concise Review: Induced Pluripotent Stem Cell Research in the Era of Precision Medicine. Stem Cells. 2017;35(3):545-50.
25. Ohnuki M, Takahashi K. Present and future challenges of induced pluripotent stem cells. Philos T R Soc B. 2015;370(1680).
26. Robinton DA, Daley GQ. The promise of induced pluripotent stem cells in research and therapy. Nature. 2012;481(7381):295-305.
27. Chen T, Wang F, Wu MY, Wang ZZ. Development of Hematopoietic Stem and Progenitor Cells From Human Pluripotent Stem Cells. J Cell Biochem. 2015;116(7):1179-89.
28. Hansen M, Varga E, Aarts C, Wust T, Kuijpers T, von Lindern M, et al. Efficient production of erythroid, megakaryocytic and myeloid cells, using single cell-derived iPSC colony differentiation. Stem Cell Res. 2018;29:232-44.
29. Lengerke C, Grauer M, Niebuhr NI, Riedt T, Kanz L, Park IH, et al. Hematopoietic development from human induced pluripotent stem cells. Ann N Y Acad Sci. 2009;1176:219-27.
30. Lim WF, Inoue-Yokoo T, Tan KS, Lai MI, Sugiyama D. Hematopoietic cell differentiation from embryonic and induced pluripotent stem cells. Stem Cell Res Ther. 2013;4(3):71.
31. Winkelstein JA, Marino MC, Johnston RB, Jr., Boyle J, Curnutte J, Gallin JI, et al. Chronic granulomatous disease. Report on a national registry of 368 patients. Medicine (Baltimore). 2000;79(3):155-69.
32. van den Berg JM, van Koppen E, Ahlin A, Belohradsky BH, Bernatowska E, Corbeel L, et al. Chronic Granulomatous Disease: The European Experience. Plos One. 2009;4(4).
33. Brault J, Goutagny E, Telugu N, Shao K, Baquie M, Satre V, et al. Optimized Generation of Functional Neutrophils and Macrophages from Patient-Specific Induced Pluripotent Stem Cells: Ex Vivo Models of X(0)-Linked, AR22(0)- and AR47(0)- Chronic Granulomatous Diseases. Biores Open Access. 2014;3(6):311-26.
34. Brault J, Vaganay G, Le Roy A, Lenormand JL, Cortes S, Stasia MJ. Therapeutic effects of proteoliposomes on X-linked chronic granulomatous disease: proof of concept using macrophages differentiated from patient-specific induced pluripotent stem cells. Int J Nanomed. 2017;12:2161-77.
35. Dreyer AK, Hoffmann D, Lachmann N, Ackermann M, Steinemann D, Timm B, et al. TALEN-mediated functional correction of X-linked chronic granulomatous disease in patient-derived induced pluripotent stem cells. Biomaterials. 2015;69:191-200.
36. Flynn R, Grundmann A, Renz P, Hanseler W, James WS, Cowley SA, et al. CRISPR-mediated genotypic and phenotypic correction of a chronic granulomatous disease mutation in human iPS cells. Exp Hematol. 2015;43(10):838-48 e3.
37. Jiang Y, Cowley SA, Siler U, Melguizo D, Tilgner K, Browne C, et al. Derivation and Functional Analysis of Patient-Specific Induced Pluripotent Stem Cells as an In Vitro Model of Chronic Granulomatous Disease. Stem Cells. 2012;30(4):599-611.
38. Laugsch M, Rostovskaya M, Velychko S, Richter C, Zimmer A, Klink B, et al. Functional Restoration of gp91phox-Oxidase Activity by BAC Transgenesis and Gene Targeting in X-linked Chronic Granulomatous Disease iPSCs. Molecular Therapy. 2016;24(4):812-22.
39. Merling RK, Kuhns DB, Sweeney CL, Wu X, Burkett S, Chu J, et al. Gene-edited pseudogene resurrection corrects p47(phox)-deficient chronic granulomatous disease. Blood Adv. 2017;1(4):270-8.
40. Merling RK, Sweeney CL, Choi U, De Ravin SS, Myers TG, Otaizo-Carrasquero F, et al. Transgene-free iPSCs generated from small volume peripheral blood nonmobilized CD34+ cells. Blood. 2013;121(14):e98-107.

41. Merling RK, Sweeney CL, Chu J, Bodansky A, Choi U, Priel DL, et al. An AAVS1-Targeted Minigene Platform for Correction of iPSCs From All Five Types of Chronic Granulomatous Disease. Molecular Therapy. 2015;23(1):147-57.
42. Zou J, Sweeney CL, Chou BK, Choi U, Pan J, Wang H, et al. Oxidase-deficient neutrophils from X-linked chronic granulomatous disease iPS cells: functional correction by zinc finger nuclease-mediated safe harbor targeting. Blood. 2011;117(21):5561-72.
43. Brault J, Vigne B, Stasia MJ. Ex vivo models of Chronic Granulomatous Disease. Knaus UG, Leto TL, editors: Springer Nature; 2019 in press.
44. Li XJ, Grunwald D, Mathieu J, Morel F, Stasia MJ. Crucial role of two potential cytosolic regions of Nox2, (TSSTKTIRRS200)-T-191 and (484)DESQANHFAVHHDEEKD(500), on NADPH oxidase activation. J Biol Chem. 2005;280(15):14962-73.
45. Lagadinou ED, Sach A, Callahan K, Rossi RM, Neering SJ, Minhajuddin M, et al. BCL-2 Inhibition Targets Oxidative Phosphorylation and Selectively Eradicates Quiescent Human Leukemia Stem Cells. Cell Stem Cell. 2013;12(3):329-41.
46. Rodrigues-Moreira S, Moreno SG, Ghinatti G, Lewandowski D, Hoffschir F, Ferri F, et al. Low-Dose Irradiation Promotes Persistent Oxidative Stress and Decreases Self-Renewal in Hematopoietic Stem Cells. Cell Rep. 2017;20(13):3199-211.
47. Burritt JB, Fritel GN, Dahan I, Pick E, Roos D, Jesaitis AJ. Epitope identification for human neutrophil flavocytochrome b monoclonals 48 and 449. Eur J Haematol. 2000;65(6):407-13.
48. O'Neill S, Mathis M, Kovacic L, Zhang SS, Reinhardt J, Scholz D, et al. Quantitative interaction analysis permits molecular insights into functional NOX4 NADPH oxidase heterodimer assembly. J Biol Chem. 2018;293(23):8750-60.
49. Chomczynski P, Sacchi N. Single-Step Method of Rna Isolation by Acid Guanidinium Thiocyanate Phenol Chloroform Extraction. Anal Biochem. 1987;162(1):156-9.
50. Feraud O, Valogne Y, Melkus MW, Zhang YY, Oudrhiri N, Haddad R, et al. Donor Dependent Variations in Hematopoietic Differentiation among Embryonic and Induced Pluripotent Stem Cell Lines. Plos One. 2016;11(3).
51. Heo HR, Song H, Kim HR, Lee JE, Chung YG, Kim WJ, et al. Reprogramming mechanisms influence the maturation of hematopoietic progenitors from human pluripotent stem cells. Cell Death Dis. 2018;9.
52. Kyttala A, Moraghebi R, Valensisi C, Kettunen J, Andrus C, Pasumarthy KK, et al. Genetic Variability Overrides the Impact of Parental Cell Type and Determines iPSC Differentiation Potential. Stem Cell Rep. 2016;6(2):200-12.
53. Ortmann D, Vallier L. Variability of human pluripotent stem cell lines. Curr Opin Genet Dev. 2017;46:179-85.
54. Lanconi R, de Arruda RP, Alves MBR, Oliveira LZ, dos Santos GDC, Lemes KM, et al. Validation of the CellRox Deep Red (R) fluorescent probe to oxidative stress assessment in equine spermatozoa. Anim Reprod. 2017;14(2):437-41.
55. Majeti R, Park CY, Weissman IL. Identification of a hierarchy of multipotent hematopoietic progenitors in human cord blood. Cell Stem Cell. 2007;1(6):635-45.
56. Notta F, Doulatov S, Laurenti E, Poeppl A, Jurisica I, Dick JE. Isolation of Single Human Hematopoietic Stem Cells Capable of Long-Term Multilineage Engraftment. Science. 2011;333(6039):218-21.
57. Ogawa M, Matsuzaki Y, Nishikawa S, Hayashi S, Kunisada T, Sudo T, et al. Expression and function of c-kit in hemopoietic progenitor cells. J Exp Med. 1991;174(1):63-71.
58. Sumide K, Matsuoka Y, Kawamura H, Nakatsuka R, Fujioka T, Asano H, et al. A revised road map for the commitment of human cord blood CD34-negative hematopoietic stem cells. Nat Commun. 2018;9.
59. Takahashi M, Matsuoka Y, Sumide K, Nakatsuka R, Fujioka T, Kohno H, et al. CD133 is a positive marker for a distinct class of primitive human cord blood-derived CD34-negative hematopoietic stem cells. Leukemia. 2014;28(6):1308-15.

60. Yin AH, Miraglia S, Zanjani ED, Almeida-Porada G, Ogawa M, Leary AG, et al. AC133, a novel marker for human hematopoietic stem and progenitor cells. Blood. 1997;90(12):5002-12.
61. Kollet O, Spiegel A, Peled A, Petit I, Byk T, Hershkoviz R, et al. Rapid and efficient homing of human CD34(+)CD38(-/low)CXCR4(+) stem and progenitor cells to the bone marrow and spleen of NOD/SCID and NOD/SCID/B2m(null) mice. Blood. 2001;97(10):3283-91.
62. Genovese P, Schiroli G, Escobar G, Di Tomaso T, Firrito C, Calabria A, et al. Targeted genome editing in human repopulating haematopoietic stem cells. Nature. 2014;510(7504):235-+.
63. Kardel MD, Eaves CJ. Modeling human hematopoietic cell development from pluripotent stem cells. Experimental Hematology. 2012;40(8):601-11.
64. Choi KD, Vodyanik M, Slukvin II. Hematopoietic differentiation and production of mature myeloid cells from human pluripotent stem cells. Nat Protoc. 2011;6(3).
65. Vodyanik MA, Bork JA, Thomson JA, Slukvin II. Human embryonic stem cell-derived CD34(+) cells: efficient production in the coculture with OP9 stromal cells and analysis of lymphohematopoietic potential. Blood. 2005;105(2):617-26.
66. Vodyanik MA, Slukvin, II. Hematoendothelial differentiation of human embryonic stem cells. Curr Protoc Cell Biol. 2007;Chapter 23:Unit 23 6.
67. Nayernia Z, Colaianna M, Robledinos-Anton N, Gutzwiller E, Sloan-Bena F, Stathaki E, et al. Decreased neural precursor cell pool in NADPH oxidase 2-deficiency: From mouse brain to neural differentiation of patient derived iPSC. Redox Biology. 2017;13:82-93.
68. Kang XL, Wei XX, Jiang L, Niu C, Zhang JY, Chen SF, et al. Nox2 and Nox4 Regulate Self-Renewal of Murine Induced-Pluripotent Stem Cells. Iubmb Life. 2016;68(12):963-70.
69. Xiao QZ, Luo ZL, Pepe AE, Margariti A, Zeng LF, Xu QB. Embryonic stem cell differentiation into smooth muscle cells is mediated by Nox4-produced H2O2. Am J Physiol-Cell Ph. 2009;296(4):C711-C23.
70. Li J, Stouffs M, Serrander L, Banfi B, Bettiol E, Charnay Y, et al. The NADPH oxidase NOX4 drives cardiac differentiation: Role in regulating cardiac transcription factors and MAP kinase activation. Mol Biol Cell. 2006;17(9):3978-88.
71. Topchiy E, Panzhinskiy E, Griffin WST, Barger SW, Das M, Zawada WM. Nox4-Generated Superoxide Drives Angiotensin II-Induced Neural Stem Cell Proliferation. Dev Neurosci-Basel. 2013;35(4):293-305.
72. Fan J, Cai H, Tan WS. Role of the plasma membrane ROS-generating NADPH oxidase in CD34(+) progenitor cells preservation by hypoxia. J Biotechnol. 2007;130(4):455-62.
73. Hole PS, Zabkiewicz J, Munje C, Newton Z, Pearn L, White P, et al. Overproduction of NOX-derived ROS in AML promotes proliferation and is associated with defective oxidative stress signaling. Blood. 2013;122(19):3322-30.
74. Baehner RL, Millar-Groff S, Bringas P. Developmental expression of NADPH phagocytic oxidase components in mouse embryos. Pediatr Res. 1999;46(2):152-7.
75. Vlaski-Lafarge M, Ivanovic Z. Reliability of ROS and RNS detection in hematopoietic stem cells - potential issues with probes and target cell population. J Cell Sci. 2015;128(21):3849-60.
76. Diez B, Genovese P, Roman-Rodriguez FJ, Alvarez L, Schiroli G, Ugalde L, et al. Therapeutic gene editing in CD34(+) hematopoietic progenitors from Fanconi anemia patients. EMBO Mol Med. 2017;9(11):1574-88.
77. Fali T, Fabre-Mersseman V, Yamamoto T, Bayard C, Papagno L, Fastenackels S, et al. Elderly human hematopoietic progenitor cells express cellular senescence markers and are more susceptible to pyroptosis. JCI Insight. 2018;3(13).
78. Folkerts H, Hilgendorf S, Wierenga ATJ, Jaques J, Mulder AB, Coffer PJ, et al. Inhibition of autophagy as a treatment strategy for p53 wild-type acute myeloid leukemia. Cell Death Dis. 2017;8.
79. Kaufman DS, Hanson ET, Lewis RL, Auerbach R, Thomson JA. Hematopoietic colony-forming cells derived from human embryonic stem cells. P Natl Acad Sci USA. 2001;98(19):10716-21.
80. Kennedy M, D'Souza SL, Lynch-Kattman M, Schwantz S, Keller G. Development of the hemangioblast defines the onset of hematopoiesis in human ES cell differentiation cultures. Blood. 2007;109(7):2679-87.

81. Ledran MH, Krassowska A, Armstrong L, Dimmick I, Renstrom J, Lang R, et al. Efficient hematopoietic differentiation of human embryonic stem cells on stromal cells derived from hematopoietic niches. Cell Stem Cell. 2008;3(1):85-98.
82. Handgretinger R, Gordon PR, Leimig T, Chen XH, Buhring HJ, Niethammer D, et al. Biology and plasticity of CD133(+) hematopoietic stem cells. Ann Ny Acad Sci. 2003;996:141-51.
83. Kobari L, Giarratana MC, Pflumio F, Izac B, Coulombel L, Douay L. CD133(+) cell selection is an alternative to CD34(+) cell selection for ex vivo expansion of hematopoietic stem cells. J Hematoth Stem Cell. 2001;10(2):273-81.
84. Anderson NJ, Bhatia R. Enhanced engraftment and maintenance of CXCR4 expressing CD34+cells in vivo is related to microenvironmental interactions, rather than direct receptor signaling to hernatopoietic stem cells. Blood. 2005;106(11):649a-a.
85. Shultz LD, Keck J, Burzenski L, Jangalwe S, Vaidya S, Greiner DL, et al. Humanized mouse models of immunological diseases and precision medicine. Mamm Genome. 2019.
86. Amabile G, Welner RS, Nombela-Arrieta C, D'Alise AM, Di Ruscio A, Ebralidze AK, et al. In vivo generation of transplantable human hematopoietic cells from induced pluripotent stem cells. Blood. 2013;121(8):1255-64.
87. Suzuki N, Yamazaki S, Yamaguchi T, Okabe M, Masaki H, Takaki S, et al. Generation of Engraftable Hematopoietic Stem Cells From Induced Pluripotent Stem Cells by Way of Teratoma Formation. Molecular Therapy. 2013;21(7):1424-31.
88. Chen C, Liu Y, Liu RH, Ikenoue T, Guan KL, Liu Y, et al. TSC-mTOR maintains quiescence and function of hematopoietic stem cells by repressing mitochondrial biogenesis and reactive oxygen species. Journal of Experimental Medicine. 2008;205(10):2397-408.
89. Hamid ZA, Tan HY, Chow PW, Harto KAW, Chan CY, Mohamed J. The Role of N-Acetylcysteine Supplementation on the Oxidative Stress Levels, Genotoxicity and Lineage Commitment Potential of Ex Vivo Murine Haematopoietic Stem/Progenitor Cells. Sultan Qaboos Univ Med J. 2018;18(2):e130-e6.
90. Jang YY, Sharkis SJ. A low level of reactive oxygen species selects for primitive hematopoietic stem cells that may reside in the low-oxygenic niche. Blood. 2007;110(8):3056-63.
91. Zou J, Zou P, Lou Y, Xiao Y, Wang J, Liu LB. The Cross-talk between ROS and p38MAPK alpha in the Ex Vivo Expanded Human Umbilical Cord Blood CD133(+) Cells. J Huazhong U Sci-Med. 2011;31(5):591-5.
92. Lee J, Dykstra B, Sackstein R, Rossi DJ. Progress and obstacles towards generating hematopoietic stem cells from pluripotent stem cells. Current Opinion in Hematology. 2015;22(4):317-23.
93. Sugimura R, Jha DK, Han A, Soria-Valles C, da Rocha EL, Lu YF, et al. Haematopoietic stem and progenitor cells from human pluripotent stem cells. Nature. 2017;545(7655):432-+.
94. Sekhsaria S, Fleisher TA, Vowells S, Brown M, Miller J, Gordon I, et al. Granulocyte colony-stimulating factor recruitment of CD34+ progenitors to peripheral blood: impaired mobilization in chronic granulomatous disease and adenosine deaminase--deficient severe combined immunodeficiency disease patients. Blood. 1996;88(3):1104-12.